OVEREXPRESSION OF ADENYLATE CYCLASE ISOFORMS ALTERS CELL SIGNALING PATHWAYS IN NF1-NULL MALIGNANT PERIPHERAL NERVE SHEATH TUMORS

by

JoAnna Hughes

M.S. (Shippensburg University) 2007

THESIS

Submitted in partial satisfaction of the requirements

for the degree of

MASTER OF SCIENCE

in

BIOMEDICAL SCIENCE

in the

GRADUATE SCHOOL

of

HOOD COLLEGE

November 2017

Accepted:

Ricky R. Hirschhorn, Ph.D. Committee Member	Ann L. Boyd, Ph.D. Director, Biomedical Science Program
Jeffrey Rossio, Ph.D. Committee Member	
Georgette N. Jones, Ph.D. Thesis Adviser	April M. Boulton, Ph.D. Interim Dean of the Graduate School

STATEMENT OF USE AND COPYRIGHT WAIVER

I authorize Hood College to lend this thesis, or reproductions of it, in total or in part, at the request of other institutions or individuals for the purpose of scholarly research.

DEDICATION

I would like to dedicate this study to Joyce, Michelle, Michael, and Kayla.

ACKNOWLEDGEMENTS

First and foremost, I would like to thank my family. My Mom and Dad have been there from before day one (imagine that), making sure I had the resources to learn – even if that meant dissecting one of the fish from the tank on the cutting board (Sorry, Mom. Thanks, Dad for the lesson on how fish worked.). My dog, Soup, provided so many cuddles when I needed it. And of course, I need to thank my wife, Nicole, for supporting me during this journey. Her patience and flexibility while I worked evenings, weekends, and vacations went above and beyond. The glass of wine that awaited me after a less than stellar experiment was appreciated too.

I am eternally grateful to the lab of Dr. Karlyne Reilly at the National Cancer Institute (Bethesda, MD) for donating ST88-14 cells so I could complete my thesis, but most of all I need to thank the Graduate School and Biomedical Science Program of Hood College. They provided me with an incredibly solid foundation to understand and investigate this research. In addition, the faculty and staff of the Biology Department lent a helpful hand or sympathetic ear more times than I can count. I would like to extend specific thanks to Mayme Kugler, Hans Wagner, and Dr. Kathy Falkenstein. I am also grateful for James Devilbiss, my committee members, and Dr. Rachel Bagni for discussing this project with me in various stages of development. I would like to give a special nod of appreciation (and a great big mental hug) to Dr. Ricky Hirschhorn of the "Hirschhorn Foundation" for also providing me with research materials, advice, lessons about Jewish culture, and many, many laughs.

Lastly, my advisor and mentor, Dr. Georgie Jones, tolerated office pop ins, emails, texts, phone calls, and random questions in the hallway about this research, but never once did she turn me away. Most importantly, she taught me more than anyone how to apply textbook knowledge to the lab. For the first time in my life I feel like a scientist.

TABLE OF CONTENTS

ABSTRACT

The second messenger, cyclic-AMP (cAMP), is produced by ten adenylate cyclase (ADCY) isoforms. Previous studies indicate that ADCY isoforms may lead to either activation or inhibition of cAMP-dependent protein kinase (PKA), cAMP expression is increased in response to neurofibromin (*NF1)* mutations, and malignant peripheral nerve sheath tumors (MPNST) express more ADCY isoforms. ADCY expression and function are modulated by four adenosine receptors (ADORA), which have different effects on ADCY. We aimed to overexpress *ADCY 3, 6, 7*, and *9* in different cell lines to dissect the mechanism of how cAMP expression is altered after *NF1* loss.

Overexpression of *ADCY 7* significantly affected PKA activity. Overexpression of *ADCY 9* led to increased expression of *ADORA 1, 2B,* and *3* in MPNST cells. Overexpressed *ADCY 3* and *7* increased *ADORA 3* expression as well. These data indicate that changes in *ADCY* and *ADORA* expression in MPNSTs may account for changes in cAMP expression after loss of *NF1*.

LIST OF TABLES

LIST OF FIGURES

LIST OF ABBREVIATIONS

ADCY	adenylate cyclase
ADORA	adenosine receptor
AKT	activated kinase/protein kinase B
AMP	adenosine monophosphate
ANOVA	analysis of variance
ATP	adenosine triphosphate
ANRIL	anti-sense non-coding RNA in the INK4 locus
APP	amyloid-β (A4) precursor protein
BSA	bovine serum albumin
cAMP	cyclic adenosine monophosphate
CDKN2A	cyclin-dependent kinase inhibitor 2A
CML	chronic myelogenous leukemia
CSRD	cysteine-serine rich domain
CT	cycle threshold
CTD	C-terminal domain
cDNA	complementary DNA
DDAH1	dimethylarginine dimethylaminohydrolase
DMEM	Delbucco's modified eagle medium
dNTP	deoxynucleotide triphosphate
DPYSL2	dihydropyrimidinase-related protein 2
EDTA	ethylenediaminetetraacetic acid

EGTA	ethyleneglycotetraacetic acid
EGFR	epidermal growth factor
EPAC	exchange proteins regulated by cAMP
ERK	extracellular signal-related kinases
FAF2	FAS-associated factor 2
FAK	focal adhesion kinase
FBS	fetal bovine serum
GAP	GTPase-activating protein
GAPDH	glyceraldehyde 3-phosphate dehydrogenase
GDNF	glial cell derived neutrotrophic factor
GDP	guanine diphosphate
GFP	green fluorescent protein
GIST	gastrointestinal stromal tumors
GPCR	G protein coupled receptor
GRD	GAP-related domain
GRK	GPCR kinase
GTP	guanine triphosphate
GWAS	genome-wide association study
HEK	human embryonic kidney
INK4	cyclin-dependent kinase inhibitor
IP3	inositol triphosphate
JXG	juvenile xanthogranuloma
LB	Luria-Bertani broth

LIM	Lin-11, Isl-1, Mec-3
LIMK2	LIM kinase domain 2
LRPPRC	leucine-rich pentatricopeptide motif-contain protein
MAPK	mitogen activating pathway kinase
MPNST	malignant peripheral nerve sheath tumor
MSH2	DNA mismatch repair protein
NF1	neurofibromatosis/neurofibromin
OPG	optical pathway glioma
PI3K	phosphoinositide-3 kinase
PBS	phosphate buffer saline
PCR	polymerase chain reaction
PDE	phosphodiesterase
PH	pleckstrin homology
PLC	phospholipase C
PKA	cAMP-dependent protein kinase
PTEN	phosphatase and tensin homolog
qPCR	quantitative PCR
RB	retinoblastoma
RQ	relative quantity
RT-PCR	real-time PCR
SBD	syndecan binding domain
SCF	stem cell factor
shRNA	short hairpin RNA

SNP	single nucleotide polymorphism
SOC	super optimal broth
SUZ12	suppressor of zeste 12
TBD	tubulin binding domain
TNF-α	tumor necrosis factor-α
UTR	untranslated region
VCP	valosin-containing protein

INTRODUCTION

Neurofibromatosis Type 1 (NF1), also known as von Recklinghausen disease or peripheral neurofibromatosis, is an autosomal dominant condition arising from germline mutations of the *NF1* gene. These mutations afflict approximately one in every 3,000 individuals and are caused by a loss of function due to haploinsufficiency of *NF1* (Ratner and Miller 2015). NF1 is a fully penetrant, pleiotropic condition where extra pigmented regions of the skin, called café-au-lait spots, and pigmented nodules of the iris, Lisch nodules, often act as preliminary indicators (Zehavi *et al*. 1986).

The concern for individuals with NF1 is that it is a tumor predisposition syndrome where multiple tumor manifestations in glial cells of the central and peripheral nervous systems are possible. Tumor manifestations of NF1 include, but are not limited to, optical pathway gliomas (OPGs) and astrocytomas, which are commonly diagnosed in childhood, as well as juvenile chronic myelogenous leukemia (CML) and pheochromocytomas (Kalff *et al*. 1982). Other types of rare tumors include gastrointestinal stromal tumors (GIST), glomus tumors, juvenile xanthogranulomas (JXG), rhabdomyosarcomas, and lipomas (Ratner and Miller 2015).The most common tumors of those with NF1 are neurofibromas, benign tumors of Schwann cells, which can be found cutaneously, as well as subcutaneously, and can be nodular in shape or diffuse plexiforms (Ferner *et al*. 2007; Rosser and Packer 2002; Williams *et al*. 2009). Plexiform neurofibromas have the ability to transition into malignant peripheral nerve sheath tumors (MPNSTs).

MPNSTs, while affiliated with NF1, are caused by sporadic mutations in 50% of cases (Anderson *et al*. 1993). These tumor cells are usually hyperdiploid and have other

genetic mutations associated with them. Loss of function of retinoblastoma (*RB*) occurs in 25% of tumors and loss of function of phosphatase and tensin homolog (*PTEN*) occurs in 50% (Mawrin *et al.* 2002). The receptor for epidermal growth factor (*EGFR*) has higher levels of amplification than normal peripheral nerve cells (Perrone *et al.* 2009). Other notable mutations include: *p53*, cyclin-dependent kinase inhibitor 2A (*CDKN2A)*, and suppressor of zeste 12 (*SUZ12)* (Kan *et al.* 2010; Legius *et al*. 1994).

NF1 and neurofibromin

To study NF1 and the various manifestations of the condition, one must understand the gene and its product, neurofibromin. The *NF1* gene, in humans, is found on chromosome 17q11.2 spanning approximately 350 kb (Barker *et al.* 1987). This gene contains sixty exons and has multiple alternatively spliced isoforms that contribute to the 2,434 documented *NF1* mutations reported on the Human Gene Mutation Database (Stenson *et al.* 2014). Splice site mutations, nonsense, missense, deletions, insertions, frameshift, and translocation mutations have all been reported. Translocation of chromosome 8q22-23 has been identified in MPNSTs and is commonly amplified (Schmidt *et al.* 2001). Most *NF1* mutations do not correlate with phenotype, with a few exceptions including an in-frame deletion of exon 17 (delAAT), which when present in NF1 patients causes a lack of cutaneous neurofibromas and severe learning disabilities (Upadhyaya *et al*. 2007).

There have been patterns of phenotypic variation identified in genome-wide association studies (GWAS). GWAS have pointed to modifier genes as contributors to phenotype (Reviewed in Jones and Reilly 2012). If offspring inherit a single nucleotide

polymorphism (SNP) of glial cell derived neurotrophic factor (*GDNF*) from the biological father, the gene interacts with *NF1* in such a way as to increase the likelihood of megacolon (Bahuau *et al.* 2001). Also, variants in antisense non-coding RNA in the cyclin-dependent kinase inhibitors (INK4) locus (*ANRIL*) have been linked to higher incidence of plexiform neurofibromas (Pasmant *et al*. 2011).

Variation in NF1 phenotypes have been linked to other factors as well. The sex of an individual, for example, has demonstrated a role in causing tumor variations. Women have a higher risk of malignant brain tumors than men due to germline mutations that may occur during meiosis. Patterns of inheritance have also been established in phenotypes. The likelihood of a child manifesting both neurofibromas and Lisch nodules is much higher with a father who has NF1 (Lazaro *et al*. 1996). In addition, DNA methylation has been studied as a reason for variation. Studies of monozygotic twins with NF1 were found to have varied levels of methylation of the 5' UTR promoter and exon one, which caused slightly different phenotypes between the twins (Harder *et al.* 2010). In a separate study, promoter methylation was found to decrease expression of DNA mismatch repair protein (*MSH2*), this may lead to conditions that favor tumor development (Reviewed in Jones and Reilly 2012).

Neurofibromin's known splice variants may impact its protein structure. Some pre-mRNA variations alter the reading frame (most commonly, exon 23, 29 and 30) and may lead to truncated proteins (Barron and Lou 2012). Of these proteins, The National Center for Biotechnology Information (NCBI) catalogues two isoforms for neurofibromin (NP_001035957.1 and NP_000258.1) that are 2,839 and 2,818 amino acids in length, but each contain the same seven domains (Ercolino *et al.* 2014; Ratner and Miller 2015). The

N-terminus of neurofibromin has a cysteine-serine rich domain (CSRD), which can be phosphorylated by cAMP-dependent protein kinsase (PKA) at threonine (Thr) residue 586 and serine (Ser) residues 818 and 876 (Figure 1) (Tokuo *et al*. 2001). The CSRD is also a binding site for dimethylarginine dimethylaminohydrolase (DDAH1), a known regulator of nitric oxide signaling (Izawa *et al.* 1996; Tokuo *et al.* 2001). Moving towards the C-terminus is the tubulin-binding domain (TBD), which uses tubulin and leucine-rich pentatricopeptide motif-contain protein (LRPPRC) for intracellular trafficking (Bollag *et al.* 1993). Of particular importance to NF1 is the GAP related domain (GRD). This domain has multiple functions: it is associated with an amyloid-β (A4) precursor protein (APP) for intracellular trafficking, aids in cell adhesions with syndecan (also occurs at the C-terminal syndecan binding domain (SBD)), can stimulate ubiquitinylation via FAS-associated factor 2 (FAF2), and has the Ras binding location (Hsueh *et al.* 2001). Due to neurofibromin's relationship with Ras, it can act as a tumor suppressor regulating the RAS-GTP active state *(*Basu *et al.* 1992*;* Xu *et al.* 1990). The GRD is a highly conserved region where different missense mutations, and a splice variant of exon 23, cause the GRD to lose its function and, as a consequence, its downstream signaling (Ratner and Miller 2015; Upadhyaya *et al.* 2007). The SEC14 and Pleckstrin homology (PH) domains are very similar because they both stimulate ubiquitinylation via Lin-11, Isl-1, Mec-3 (LIM) kinase domain 2 (LIMK2) and they stimulate neuronal differentiation through valosin-containing protein (VCP) (Endo *et al*. 2003; Wang *et al*. 2011). These two domains differ in the SEC14 domain that binds to phospholipids for cell adhesion. The carboxyl-terminal domain (CTD) also has the ability to be phosphorylated by PKA. Like the CSRD, it also has a single Thr phosphorylation site at residue 2556, but it has four

Ser residues that may be phosphorylated: 2576, 2578, 2580, and 2813 (Tokuo *et al.* 2001). Futhermore, the CTD has binding sites for DDAH1 and 14-3-3 for cell signaling, focal adhesion kinase (FAK) which aids in the communication for cell migration, ubiquitinylation through stem cell factor (SCF), and promotes neuronal differentiation via interactions with dihydropyrimidinase-related protein 2 (DPYSL2) (Izawa *et al.* 1996; Kweh *et al.* 2009; Ratner and Miller 2015; Tokuo *et al*. 2001; Zachary 1997).

Figure 1: The seven domains of neurofibromin. Beginning with the N-terminus: CSRD (Cystein-Serine Repeat Doman), TBD (Tubulin Binding Domain), GRD (in green) (GAP Related Domain), SEC14 domain, PH (Pleckstrin Homology domain), CTD (C-Terminus Domain), and SBD (Syndecan Binding Domain). The pink domains indicate regions of known PKA phosphorylation. The two isoforms of neurofibromin are 2,818 and 2,839 amino acids in length (Ercolino *et al.* 2014; Ratner and Miller 2015; Tokuo *et al.* 2001).

Neurofibromin can be detected through DNA, mRNA, or protein analysis. Normal cells of neural crest origin, like peripheral nerves, express high levels of NF1 (Anderson *et al*. 1993). However, NF1 has been detected in numerous different cell types outside of peripheral nerves, including human embryonic kidney (HEK293), white blood cells, skin fibroblasts, brain, spleen, skeletal muscle, and many types of cancers outside of MPNSTs (Kweh *et al.* 2009; Wallace *et al.* 1990).

Adenosine receptors

Adenosine is a purine nucleotide that is found intracellularly and extracellularly. Intracellular adenosine is formed when adenosine monophosphate (AMP) is

dephosphorylated by 5'-nucleotidase or by hydrolysis of *S*-adenosyl-homocysteine (Broch and Ueland 1980). The dephosphorylation of ATP to ADP also uses these molecules. Adenosine, within the cell, is transported to the exterior via facilitative diffusion, although different tissues do have different concentration gradients. Once extracellular adenosine is highly concentrated, it is transported inside the cell and is phosphorylated into AMP (Fredholm *et al*. 2001)

Adenosine is the primary ligand that binds to adenosine receptors (ADORA) to induce signaling cascades (inosine also may bind). ADORAs are G protein coupled receptors (GPCR) that have asparginine-linked glycoproteins as part of their structure. There are four identified sub-types of ADORA in humans and have structural, as well as functional, differences between them (Collin and Hourani 1993). *ADORA 1* and *3* share 49% genetic similarity, whereas *ADORA 2A* and *2B* share 59% homology (Jacobson and Gao 2006). ADORA 1, ADORA 2B, and ADORA 3 proteins all have sites for palmitoylation at the C-terminus, whereas ADORA 2A does not (Linden 2001). When ADORA 3 is depalmitoylated it is more prone to be phosphorylated by G protein-coupled receptor kinases (GRKs) (Palmer and Stiles 2000). ADORA 3 also lacks histidine residues at its ligand recognition site (Fredholm *et al*. 2001). Variations in these structures are why the receptors respond differently to assays and tools used to study them.

ADORA receptors also differ in their genetic loci, protein size, tissues expression, and their relationship with G proteins, specifically adenylate cyclase (ADCY), the enzyme that catalyzes ATP into cyclic-AMP (cAMP). ADORA 1 is found on chromosome 1q32.1 and the protein is 326 amino acids. This receptor is found in its

highest concentrations in the brain's cortex, spinal cord, adrenal glands, and eyes (Fredholm *et al*. 2001). It is a G protein inhibitor, thus it inhibits ADCY, causing cAMP levels to decrease. ADORA 2A and 2B are both stimulators of G proteins; therefore, associated with increases in cAMP. ADORA 2A is found on chromosome 22p11.2, averages 410 amino acids (this receptor is polymorphic), and is found in highest concentrations in the spleen, thymus, leukocytes, and platelets (Fredholm *et al*. 2001). ADORA 2B is found on chromosome 17p12-11.2, is 328 amino acids in length, and is found in the highest concentrations in the cecum, colon, and bladder (Fredholm *et al*. 2001). ADORA 3 is found on chromosome 1p21-13, is the smallest receptor (318 amino acids), inhibits G proteins, and is found in much lower quantities than the other receptors. However, ADORA 3 is found in the heart and is influential in mast cell degranulation (Fredholm *et al*. 2001; da Rocha Lapa *et al.* 2014). Lastly, it should be noted that ADORA 2A, 2B, and 3 also respond to inosine, an adenosine metabolite, to initiate signaling cascades (da Rocha Lapa *et al.* 2014).

Aside from G proteins, ADORA initiates signal cascades for other molecules as well (Figure 2). Phospholipase C (PLC), an enzyme that removes phospholipids from phosphate(s), is stimulated by ADORA 1 and ADORA 2B (Becker *et al.* 2012, da La Rocha *et al.* 2014). Once stimulated, PLC continues the cascade to inositol triphosphate (IP3) and as a consequence increases Ca^{2+} levels in the cell. Mitogen-activated protein kinases (MAPK) are also stimulated by ADORA 1 and ADORA 2B and continue to the extracellular signal-regulated kinases (ERK pathway), which is a common cell proliferation pathway. ADORA 3 stimulates phosophoinositide-3 kinase (PI3K), which

continues on to the protein kinase B (Akt)/mTOR pathway, for cell cycle regulation (Becker *et al*. 2012; da Rocha Lapa *et al*. 2014).

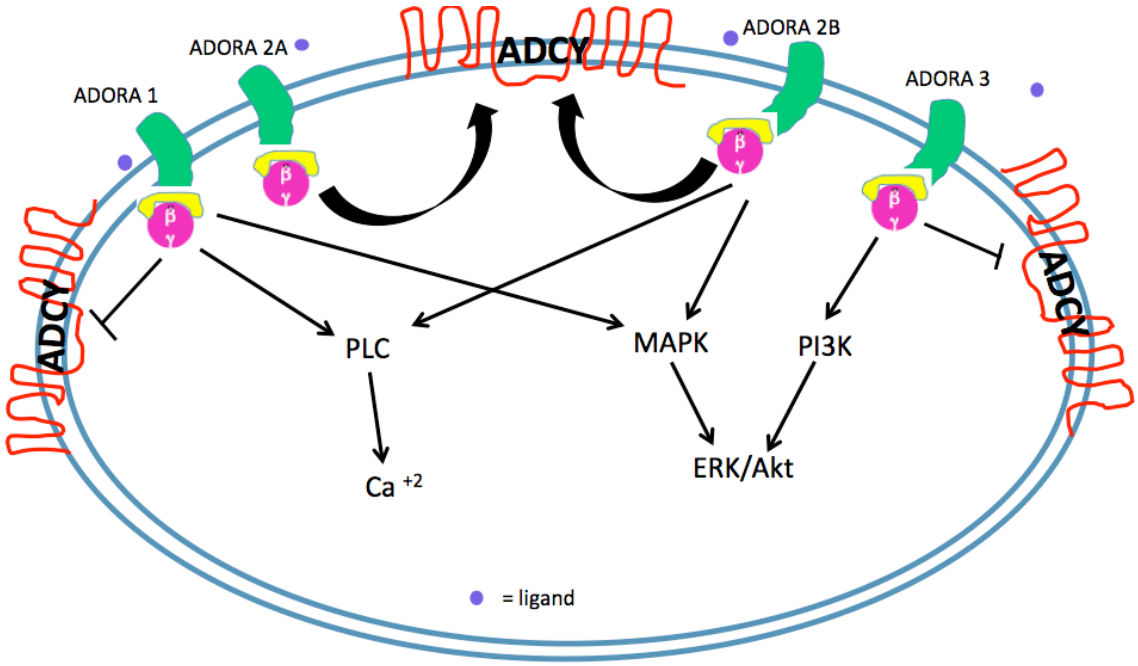

Figure 2: Isoform-specific adenosine receptor (ADORA) activation yields distinct signal cascades after a ligand binds. The ligand is usually adenosine, but may be inosine. All receptors, for the exception of ADORA 1, lead to ERK/Akt.

Adenylate cyclase and cyclic-AMP

In humans, there are nine isoforms of the enzyme adenylate cyclase (ADCY) that share 60% amino acid sequence homology. The differences in sequence cause a molecular weight range of 119 to 175-kDa; however, they all share the same structure of two, six transmembrane cassettes with their N-terminus and C-terminus residing in the cytoplasm (Cooper and Tabbasum 2014; Sunahara *et al*. 1996) (Figure 2). Despite the similarities between isoforms, they are divided into categories based on additional external signaling and their sequences (Ludwig and Seuwen 2002). ADCY 1, 3, and 8

produce cAMP when Ca^{2+}/calmodulin is present; ADCY 2, 4, and 7 can be activated by the β subunit of the GPCR and are not stimulated by Ca^{2+}; ADCY 5 and 6 demonstrate inhibition by low concentrations of Ca^{2+} and are PKA inhibitors; and ADCY 9 is inhibited by Ca^{2+}/calcineurin (Defer *et al.* 2000). Tissue specificity of ADCY expression, under varying conditions, leads to altered isoform expression (Defer *et al.* 2000; Ludwig and Seuwen 2002). For example, skeletal muscle only expresses ADCY 1, 3, and 9, while the spleen produces all isoforms with the exception of ADCY 8 (Ludwig and Seuwen 2002). It should be noted, that there is a tenth isoform that is soluble (sAC), rather than transmembrane, and is normally confined to the testis (Defer *et al*. 2000).

As stated before, the role of ADCY is to produce cyclic-AMP. This enzyme catalyzes the conversion of ATP into 3'-5'-cAMP (Cryer *et al.* 1969). Adenylate cyclase will produce cAMP when activated by ADORA; however, this cAMP production can be influenced by the GPCR's placement within lipid raft domains or crosstalk with other molecules (Ludwig and Seuwen 2002; Ostrom and Insel 2004). Cyclic-AMP production can further be regulated by phosphodiesterases (PDEs) and neurofibromin. Mammalian cells that have a loss of function of *NF1* increase production of cAMP (Kim *et al.* 2001). Cyclic-AMP is a second messenger required for a wide variety of cell signaling (activator or inhibitor) and plays especially influential roles in signaling exchange proteins regulated by cAMP (EPACs) and cAMP-dependent protein kinase PKA (Borland *et al*. 2009).

cAMP-Dependent Protein Kinase

Cyclic-AMP-dependent protein kinase (PKA) is a heterotetromeric holoenzyme complex consisting of two regulatory subunits bound to two inactive catalytic subunits. For the catalytic subunits to become activated and phosphorylate serine-threonine residues (like those on neurofibromin), two molecules of cAMP must cooperatively bind to each of the regulatory subunits of PKA. The bonding of cAMP induces a conformational change in the regulatory subunits and causes the catalytic subunits to be released (Tasken *et al*. 1996).

Of particular importance to this study is the signaling relationship cAMP has with the Ras, Raf, MEK/ERK pathway and PKA. PKA has the ability to stop Ras-dependent signaling because it is an inhibitor of Raf (Cook and McCormick 1993). It has been suggested that there is an inverse relationship between cAMP and Raf1 kinase levels because cAMP is simultaneously activating PKA (Mischak *et al.* 1996). For neurofibromin to function as a regulator of Ras, the CSRD and CTD need to be phosphorylated by PKA; however, PKA, is regulated by other proteins, such as 14-3-3 (Feng *et al*. 2004). It was concluded by Feng *et al.* (2004) that 14-3-3 kept Ras in its active state despite the presence of PKA. In other studies investigating the link between PKA and Ras, Ras activation was observed in cortical neurons after cAMP activation was prompted and PKA was able to mediate cAMP activity (Ambrosini *et al.* 2000). To summarize, the relationship that exists between NF1, ADORA, ADCY, cAMP, and PKA is complex and open to further investigation.

Rationale

Drosophila and mouse studies have suggested that the differences in signaling and cAMP-PKA expression between $Nf1^{+/+}$ and $Nf1^{-/-}$ may affect phenotype (Guo *et al.* 2000; Kim *et al*. 2001; The et al. 1997). Murine Schwann cells of both heterozygous and *Nf1*-null genotypes were analyzed for levels of cAMP and compared to wild type mice. Mice that were $Nf1^{-/-}$ had cAMP levels over three times higher than wild type and $Nf1^{+/-}$ had 63% more cAMP than wild type (Kim *et al.* 2001). In addition, a study of mice lacking *Prkar1a*, a gene that encodes a regulatory subunit of PKA, showed that constitutive PKA activity resulted in complete loss of Nf1 protein production in Schwann cells (Jones *et al*. 2008). Taken together, these data indicate a possible feedback signaling loop involving neurofibromin, cAMP, and PKA.

Studies conducted in *Drosophila* demonstrated that the cDNA of *NF1* is, on average, 60% homologous to human *NF1* (the GRD region is 69% homologous). *Drosophila* deficient for *NF1* were found to be smaller in size (length, wing, and eye) and suffered delayed responses to environmental stimuli (The *et al.* 1997). There were no abnormalities detected from an increase in Ras1 levels. However, these flies were saved from their deleterious phenotypes by providing them with excessive PKA (The *et al.* 1997). Lastly, in *Drosophila,* neurofibromin is required for adenylate cyclase activity in the neurons responsible for learning (Guo *et al.* 2000). It has been suggested that the learning disabilities of humans with NF1 may be caused from signaling issues rather than from a greater developmental problem (Davis 2000).

In a 2011 study, Dang and DeVries investigated cAMP metabolism in humans as it related to MPNST cells. They compared wild type $NF1^{+/+}$ human Schwann cells to two

different MPNST (*NF1*$^{+/-}$) cell lines, ST88-14 and T265. Using quantitative polymerase chain reaction (qPCR), the wild type Schwann cells showed strong expression of *ADCY 3, 4, 9*, and weak expression of *ADCY 7*. The two MPNST cells lines expressed the same isoforms as wild type plus *ADCY 2, 5,* and *8*. The sum cAMP level of all ADCY isoforms was assessed using ELISA and the results showed that wild type cells produced approximately half the cAMP as compared to MPNST cells. This suggests that the excessive cAMP level is more than enough to activate PKA, and to influence other types of cell signaling downstream from cAMP, such as the Ras-Raf-ERK/MEK pathway (Cook and McCormick 1993). Futhermore, it suggests that ADORA could be indirectly stimulated by increases in specific ADCY isoforms because of the involvement of cAMP in multiple cellular pathways.

The goal for this study is to dissect the relationship between ADCY, ADORA, and PKA in the context of mutated *NF1* by determining if ADCY directs neurofibromin or neurofibromin directs ADCY. It is also hypothesized, that overexpression of *ADCY* will increase *ADORA* expression. Support for these hypotheses could lead to different treatment options for patients with NF1, such as those that focus on inhibiting cAMP activity. This would be a significant change from one glioblastoma treatment strategy that focuses on increasing cAMP activity with Rolipram, a PDE inhibitor (Yang *et al.* 2007). While PDE inhibitors have demonstrated delayed growth in some human tumors; they have also been shown to increase proliferation in melanoma (Chiaradonna *et al*. 2008). It should be noted that melanocytes, like Schwann cells, are neural crest derived and prone to altered function in NF1 patients (Anderson *et al*. 1993). Targeting ADORA is also not unheard of in cancer treatment. ADORA 3 activation has been targeted in colon cancer

because of its ability to signal and control cell proliferation and ADORA 2A has been examined because of its signaling in apoptotic mechanisms (Jacobson and Gao 2006). This study may provide support to the notion that tumors of the peripheral nervous system need to be treated in a manner that is different from the treatment strategies for the central nervous system or other cancers, in general.

MATERIALS AND METHODS

Cell culture, counting, and harvesting

Human embryonic kidney (HEK293T, CRL-11268) cells were purchased from American Type Culture Collection (ATCC) (Manassas, VA) and cultured in Delbucco's Modified Eagle's Medium (DMEM) containing 4.5 g/L D-Glucose with added L-Glutamine and sodium pyruvate (Cellgro, Corning, Manassas, VA) and modified with 10% heat-inactivated Fetal Bovine Serum (FBS) (HyClone, ThermoFisher, Walkersville, MD), and 1% Penicillin/Streptomycin (5000 units/mL Penicillin and 5000 μg/mL Streptomycin) (Pen/Strep) (Gibco, ThermoFisher). Cells were grown as a monolayer in $10cm^2$ culture plates (Corning, Sigma-Aldrich, St. Loius, MO) or T75 culture flasks (Corning, Sigma-Aldrich) and incubated at 37°C with 5.0% CO_2.

There were two separate MPNST cell lines used in this research. The ST88-14 cells were derived from a MPNST of the lung. The seventh passage of these cells were donated by Karlyne Reilly, Ph.D. and cultured in the same manner as the HEK293T cells. The NF1 Schwann-Like Cells (sNF96.2) cells were acquired from ATCC (Manassas, VA). Upon receipt of the fifteenth passage of the cells from ATCC, they were cultured in DMEM with added L-Glutamine and sodium pyruvate (Cellgro, Corning). The DMEM media was completed with additions of 10% non-heat-inactivated FBS and 1% Pen/Strep. Cells were grown as a monolayer in $10cm^2$ culture plates or T75 culture flasks and incubated at 37°C and 5.0% CO_2.

When cells were cultured for harvest, they were grown in T225 treated flasks with phenolic style caps (CoStar, Corning). For HEK293T and sNF96.2 cells, once the culture

flask reached approximately 80% confluency, the media was aspirated, the dish washed with 15mL 1x Dulbecco's Phosphate Buffer Saline (PBS) without calcium or magnesium (Gibco, ThermoFisher). Cells were dissociated from their culture dish using TrypLE Express with phenol red (Gibco, ThermoFisher) and then neutralized with complete DMEM media. The cell suspension was collected in a conical tube and centrifuged at 1500rpm for 5 minutes. After centrifugation, the media was aspirated, fresh media was added, and the pellet triturated to resuspend the cells.

Conversely, the ST88-14 cells were dissociated from the flask with 0.25% Trypsin with phenol red and without EDTA (Gibco, ThermoFisher) and pre-warmed to 37°C. The Trypsinized flask was placed in a 37°C and 5.0% CO_2 incubator for 5 minutes. Once the cells had lifted, the cell suspension was neutralized with complete media. Centrifugation and resuspension of ST88-14 cells followed the same procedure as the other two cell lines.

To perform cell counts, the cell suspension was mixed 1:1 with Trypan blue stain 0.4% (Gibco, ThermoFisher). The stained suspension was pipetted into both portions of a Countess cell counting chamber slide (Invitrogen, ThermoFisher). HEK293T cells were counted using HEK293T programmed (default) parameters of a Countess™ Automated Cell Counter (Invitrogen, ThermoFisher). For the MPNST cells, the parameters were kept the same, except cell length was maximized to 60μm. The live cells were averaged and this number was used to calculate how much cell volume was required to plate the appropriate number of cells for transfection.

On day three after transfection, cell culture dishes were aspirated and washed with room temperature 1x PBS twice before the cells were scraped in 1x PBS. For HEK293T and sNF96.2 cells, the suspension was aspirated and divided into two conical tubes and placed in ice. Cells were then centrifuged for five minutes at 180 x g. The PBS was carefully aspirated. Afterwards, the pellet was resuspended in either protein lysis buffer or RNA lysis buffer. Protein lysis buffer consisted of 25mM Tris-HCl, 0.5mM EDTA, 0.5mM EGTA, 10mM β-mercaptoethanol, 7x protease inhibitor, and a 100x phosphatase inhibitor. RNA lysis buffer was prepared as directed by the PureLink RNA Mini Kit (Ambion, ThermoFisher) specifications. The ST88-14 cell suspensions were not divided; all cells were stored in RNA lysis buffer. Samples were stored at -80°C if they were not immediately used for RNA extraction or the PKA assay.

Transformation and plasmid purification

DH5α subcloning efficiency competent cells (Invitrogen, ThermoFisher) were used to propagate plasmid vectors. DH5α is a common strain of *Escherichia coli* (*E. coli*) used for subcloning. These cells were transformed with MISSION control vector pKLO.1-puro-Ubc-TurboGFP plasmid (Figure 3) (Sigma-Aldrich, St. Louis, MO), and spread on ampicillin (1:1000) treated Luria-Bertani broth (LB) agar plates. Plates were left to incubate overnight at 37°C. This was the positive control for transfection.

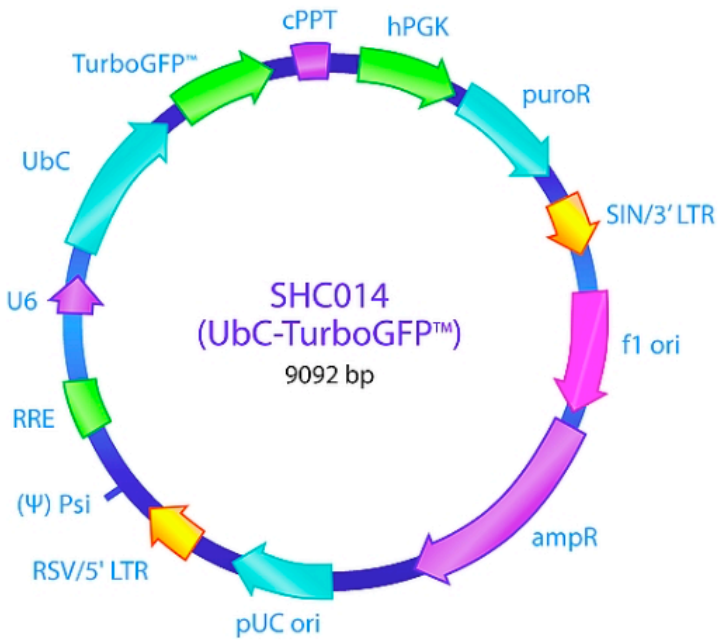

Figure 3: Plasmid map of vector SHC014 (UbC0Turbo-GFP). Plasmid map was created through PlasMapper.

After overnight growth, single bacterial colonies were selected from the plate, using aseptic techniques, and placed in 4mL LB broth with 1:1000 ampicillin. Human adenylate cyclase isoform cDNA plasmids (Dharmacon, Lafayette, CO) (Figure 5 and 6) were also propagated in this manner by adding approximately 2μL of cDNA plasmid glycerol stock to 4mL LB broth with 1:1000 ampicillin. The cultures were placed at 37°C and 2 x g on an incubated shaker overnight. After the 24-hour period, aseptic techniques were used to add 100μL of each culture to 50mL of ampicillin LB broth (1:500). These cultures were incubated at 37°C and 2 x g on a shaker for 18 hours.

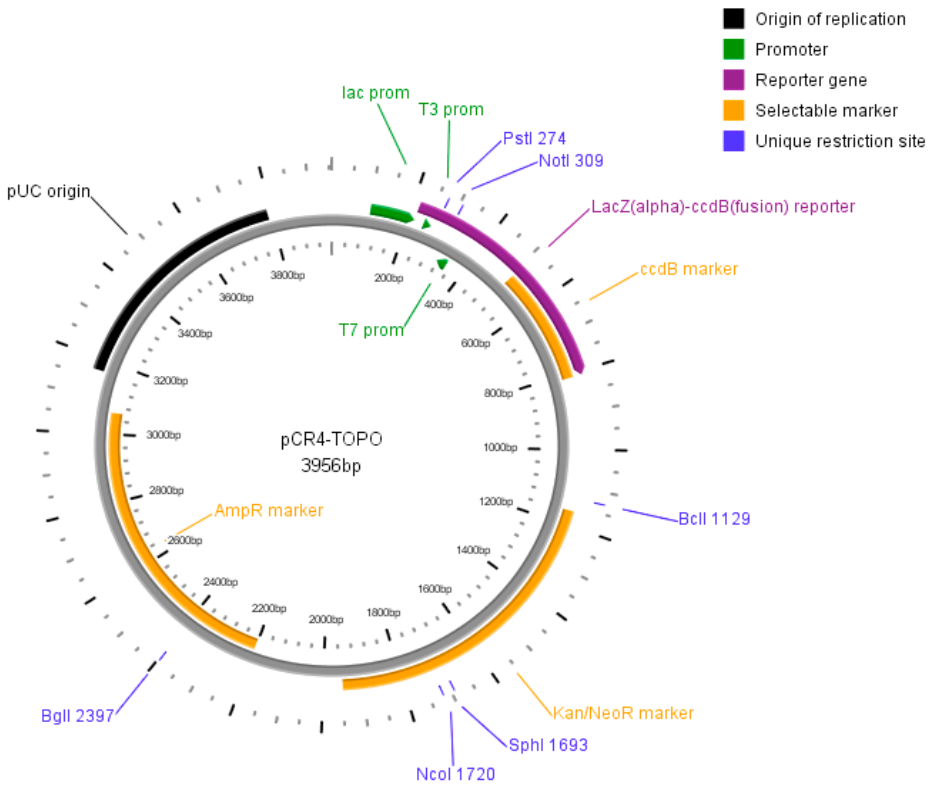

Figure 4: Plasmid map of vector pCR4-TOPO, human isoform ADCY 3. Plasmid map was created through PlasMapper. Clone ID: 8991951, Accession: BC12635 (Dharmacon, Lafayette, CO).

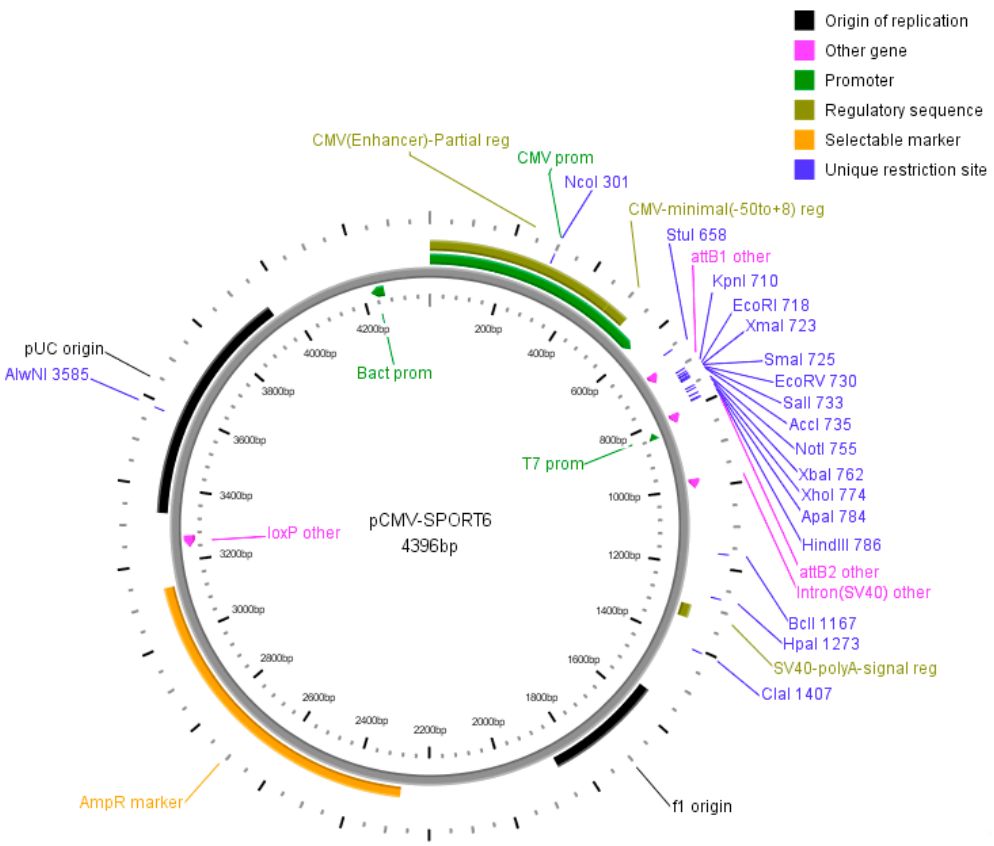

Figure 5: Plasmid map of vector pCMV-SPORT6, human ADCY isoforms 6, 7, and 9. Plasmid map was created through PlasMapper. ADCY 6, Clone ID: 6141275, Accession: BC064923. ADCY 7: Clone ID: 5211601, Accession: BC039891. ADCY 9, CloneID: 40147127, Accession: BC151207 (Dharmacon).

Plasmid DNA was extracted from the cultures and purified using the PureYield Plasmid Midiprep System (Promega, Madison, WI) via centrifugation method. Plasmids were purified according to manufacturer specifications. DNA was quantified, in triplicate, using a FLUOstar Omega microplate reader (BMG LABTECH, Cary, NC) with LVis plate and stored at +4°C.

Transfection

For HEK293T and ST88-14 cells, a cell count was performed so that each $10cm^2$ culture dish contained $3.0x10^6$ cells. For sNF96.2 cells, the cell count was $5.4x10^6$ cells, because of their slower dividing time. The cultures were then placed in an incubator programmed for 37°C and 5.0% CO_2 for 24 hours.

A master mix of 36μL Lipofectamine 2000 (Invitrogen, ThermoFisher) and 2mL of 1x Opti-MEM Reduced Serum Medium (ThermoFisher), per sample, was prepared. The untreated control contained 3mL of Opti-MEM, whereas the experimental samples contained 1.5mL Opti-MEM, 1.0μg plasmid *GFP*, and 1.0μg plasmid DNA of the targeted cDNA *ADCY* isoform. There was also a mock transfection where no plasmid DNA was added. Lipofectamine 2000 master mix was added to each plasmid DNA sample and allowed to incubate at room temperature for five minutes. After that time had lapsed, the total 3mL of solution was added slowly to the side of each appropriately labeled culture dish and then swirled to mix. The dishes were left to incubate for 24 hours at 37°C and 5.0% CO_2.

Twenty-four hours post-transfection, the transfection efficiency was determined via fluorescence microscopy. The confluency and fluorescence of each cell sample was observed in three separate locations of the culture dish to verify transfection. In the case of the ST88-14 cells, transfection efficiency was verified via Real-time PCR.

RNA extraction, cDNA synthesis, and real-time PCR

For RNA extraction, the buffered cells were vortexed and needle homogenized with a 20-gauge needle and syringe. Contents were transferred to a RNase-free tube and RNA was extracted following the PureLink RNA Mini Kit's instructions. RNA concentration was measured, in triplicate, using the LVis plate reader. RNA samples were stored at -20°C or immediately used for complementary DNA synthesis.

Complementary DNA (cDNA) synthesis was performed using the SuperScript Vilo cDNA synthesis kit (Invitrogen, ThermoFisher, Waltham, MA). For each sample, 2μg of RNA was reverse transcribed. The SuperScript kit included a 5x Reaction mix (containing primers, $MgCl_2$, and deoxynucleotide triphosphates (dNTPs)) and a 10x enzyme mix (containing reverse transcriptase and ribonuclease inhibitor). Samples were placed into a MyCycler thermal cycler (Bio-Rad Laboratories, Hercules, CA) for cDNA synthesis. Settings for thermal cycler (for denaturing, annealing, and extending) were as follows: incubation at 25°C for ten minutes, incubation at 42°C for 60 minutes, and termination at 85°C for five minutes. Temperature was held at +4°C after the synthesis was complete. All cDNA samples were treated with 5Units/μl of RNaseH (New England BioLabs, Ipswich, MA) and diluted to 2.0 ng/μl with nuclease-free water. Samples were stored at -20°C.

Gene expression was evaluated using the QuantStudio 3 Real-Time PCR System (Applied Biosystems, ThermoFisher, Waltham, MA). MicroAmp Optical 96-Well Reaction Plates (Applied Biosystems, ThermoFisher) were used to test each sample, in triplicate. Fifty percent of the sample well volume consisted of PowerUp SYBR Green

Master Mix (containing SYBR green dye, dNTPs, DNA polymerase, and ROX passive reference dye) (Applied Biosystems, Life Technologies, Austin, TX), 38% sterile distilled water, 10μM forward and 10μM reverse DNA primers (Invitrogen, ThermoFisher), and 0.08ng/μl diluted cDNA.

The *ADCY* primers selected were referenced in Ludwig and Seuwen (2002) and glyceraldehyde 3-phosphate dehydrogenase (*GAPDH*) was selected as the endogenous control gene (Table 1). Each sample was measured in triplicate. The QuantStudio 3 was programed for a Comparative cycle threshold (ΔΔCt) analysis at standard run mode with ROX as passive reference. The temperature cycles were set for the QuantStudio 3's default parameters: hold stage (50°C-95°C for 12 minutes), PCR stage (95°C – 60°C for one hour), and melt curve stage analysis. For all stages (denaturing, annealing, and extending), the rate of change for temperature was 1.6°C/s.

Table 1: DNA Primers used in Real-Time PCR for *ADCY* experiments		
Gene	Direction	Primer (5' - 3')
GAPDH	Forward	GAAGGTCGGAGTCAACGGATTT
	Reverse	ATGGGTGGAATCATATTGGAA
ADCY 1	Forward	GCGCAGCTACGAGCCGATTG
	Reverse	AGGAAGTGCTGGGCGACGTG
ADCY 2	Forward	CCGGAATGGAGGCAAACATG
	Reverse	CTACAGCCAGGTCTTATTTG
ADCY 3	Forward	CGGTGGAGAAGGAGAAGCAGAGTGG
	Reverse	CCTCCGTCTCCATCCCTGCCGTTGC
ADCY 4	Forward	GCCACCATCCTCCTTGTCTTTGCCA
	Reverse	GAGAGGAAGCCCAGCGTGCAGCAGT
ADCY 5	Forward	CTTCCTCTTCATCTGCTTTGTCCA
	Reverse	GCTGATGTTGTGCTCCTGTGCCAA
ADCY 6	Forward	GTTGCCTGTGCCCTGTTGGTCTTCT
	Reverse	GATGCCAACTGCGGTGCTATGTGCC
ADCY 7	Forward	ACTGGGTGTGTCCTTCGGGCTGGTG
	Reverse	CTCTGGAACTTGGAAAGGCATCAGG
ADCY 8	Forward	GCACTCGGCTCTGGTCCTCATCAC
	Reverse	CAGGTTCTTCAAGGGTATCGACTTG
ADCY 9	Forward	TGGGAAAGTTATTGAACGGCTG
	Reverse	CTGACATTCCCTGATGACGCTG

Before overexpression experiments began, all cells were tested for endogenous expression of all nine *ADCY* isoforms. Isoforms *3, 6, 7*, and *9* were chosen for overexpression experiments due to their expression consistency in these experiments and the Dang and DeVries (2011) study. Once overexpression of these ADCY isoforms was

confirmed, the cDNA from the cells was used to test for expression of *ADORA* isoforms. Primers for *ADORA* were taken from Sharmin *et al* (2012) and GAPDH was used as the endogenous control (Table 2).

Table 2: DNA Primers used in Real-Time PCR for *ADORA* experiments

Gene	Direction	Primer (5' -3')
GAPDH	Forward	CGGAGTCAACGGATTTGGTCGTAT
	Reverse	AGCCTTCTCCATGGTGGTGAAGAC
ADORA1	Forward	TCTGGGCGGTGAAGGTGAAC
	Reverse	AGTTGCCGTGCGTGAGGAAG
ADORA2A	Forward	TGCTTCGTCCTGGTCCTCAC
	Reverse	GCTCTCCGTCACTGCCAT
ADORA2B	Forward	CCCTTTGCCATCACCATCAG
	Reverse	CCTGACCATTCCCACTCTTGA
ADORA3	Forward	GCGCCATCTATCTTGACATCTTTT
	Reverse	CTTGGCCCAGGCATACAGG

cAMP-Dependent Protein Kinase Assay

HEK293T and sNF96.2 cells that had been suspended in protein lysis buffer were needle homogenized and then centrifuged at 16,000 x g for 10 minutes at +4°C. The supernatant was collected for protein measurement. Sample protein was measured using Bradford reagent and 2μg/μl bovine serum albumin (BSA) as a standard. Approximately 200μl samples were loaded in a 96-well microplate; BSA standard concentrations ranged from 0.0-8.0μg/μl and 1μl of each sample was assayed. The FLUOstar Omega microplate reader was set for an absorbance of 595nm. Sample protein concentrations were determined via standard curve generated from BSA standards. Protein samples were then

used in the Promega PepTag^{R} Assay for Non-radioactive Detection of cAMP-Dependent Protein Kinase (PKA) assay (Promega, Madison, WI) or stored at -80°C.

For the PKA assay, all samples were prepared per the manufacturers guidelines and contained 5x PKA Reaction buffer (Tris-HCl, $MgCl_2$, and ATP), A1 Peptide (0.4μg/μl), PKA Activator 5x solution (5μM cAMP), and distilled water. The A1 Peptide is a synthetic, oligopeptide substrate for PKA. When PKA is active it phosphorylates the oligopeptide, thus changing its charge. The positive control also contained PKA catalytic subunit and PKA dilution buffer (350mM K_3PO_4 (pH 6.8) and β-mercaptoethanol) (2μg/ml). Experimental samples between separate experiments varied in protein sample concentration; however, each individual experiment was kept consistent by using the lowest protein yield of the experiment for each sample. The protein concentration used for the three HEK293T trials was 10μg/μl and for the three trials of sNF96.2 was a range of 2μg/μl-5μg/ml. Samples were then loaded into the center of a pre-prepared 0.8% agarose gel in 50mM Tris-HCl. Gel electrophoresis was run at 45V for approximately 45 minutes. During the migration, non-phosphorylated protein moved towards the anode and phosphorylated protein moved towards the cathode of the gel apparatus (Figure 6).

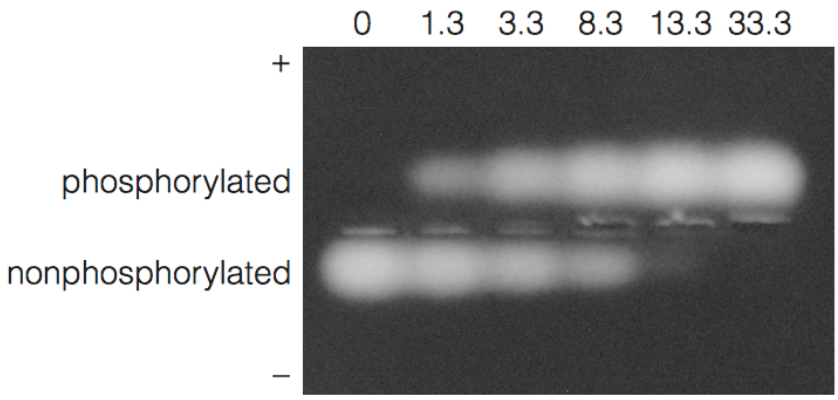

Figure 6: PKA activity assay gel showing fluorescence of the oligopeptide target of PKA under increasing PKA activity (ng/µl). Active PKA catalytic protein phosphorylates the fluorescent oligopeptide target in the assay, thereby causing a change in charge that is visualized by migration at either the anode or cathode (image from technical manual of Promega PepTag Non-Radioactive PKA assay).

The gel was analyzed for phosphorylation using a GeneSys Imager (Genesys, Daly City, CA) and its accompanying software. Images were not altered for brightness to decrease bias between experiments. When possible, two gels were run simultaneously to also decrease bias. The dot blot method was used to select fluoresced sample areas and background interference was subtracted from this value. Taking the net fluorescence, followed by dividing the protein concentration of each sample, normalized samples. This created a value to standardize the trials of sNF96.2 cells that had differing amounts of protein. The standardized data were then compared to the mock transfection, creating a ratio to compare all samples.

RESULTS

Validation of endogenous gene expression and overexpression of *ADCY* by Real Time-PCR

All untreated cells were tested for endogenous expression of *ADCY* isoforms one through nine using Real-time PCR and their results were normalized to *GAPDH*. Three trials were completed, each in triplicate, for all cell lines (Figure 7). Because this experiment was only testing for endogenous expression levels a comparative cycle threshold (ΔΔCt) analysis was chosen. The calculation of this value creates an inverse relationship; therefore, the higher the Ct value, the lower the expression. Ct values below 28 were considered "reliable" for these experiments.

HEK293T cells, the experimental control cell line, and the two MPNST cell lines had differences in expression. HEK293T had the highest expression (lower Ct values) of *ADCY 3, 6,* and *9*. There was variability between MPNST cell lines. The sNF96.2 cells also had highest expression in *ADCY 3, 6,* and *9,* but the ST88-14 cells had highest expression in *ADCY 1, 3*, and *9*. *ADCY 3, 6, 7*, and *9* were chosen for overexpression experiments because of their lower Ct (and more reliable) endogenous expression levels and lower standard deviations. This experiment also confirms the data of Dang and DeVries study, which analyzed mRNA expression of *ADCY* used ST88-14 cells and another MPNST cell line, T265 (2011).

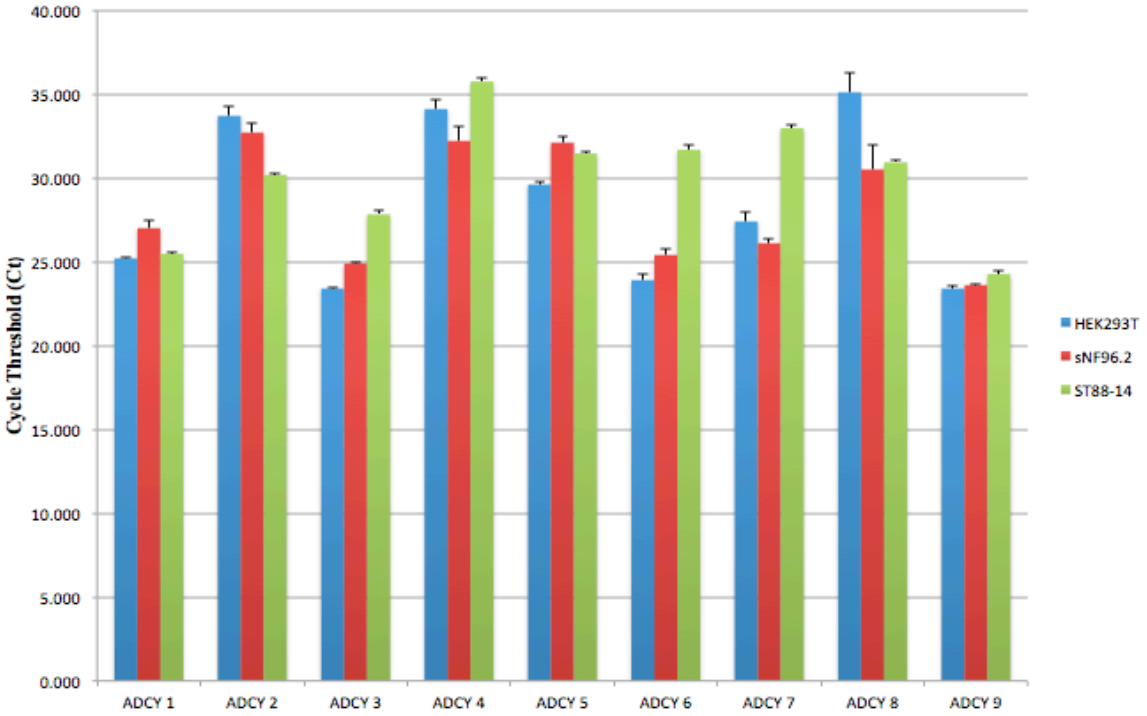

Figure 7: The cycle threshold (Ct) of *ADCY* endogenous expression in different cell lines. Each cell line was analyzed for endogenous expression of all nine transmembrane *ADCY* isoforms by Real-Time PCR. Ct values are inversely related to expression. Error bars represent standard deviation.

Once the four *ADCY* isoforms were overexpressed, it was verified through Real-time PCR relative quantity (RQ) calculation that the transfected cells only overexpressed the intended isoform (Table 3a-c). To calculate RQ, the Ct of the sample was compared against the Ct of the mock transfection. By definition the RQ value of the mock transfection is always one; therefore, values higher than one indicate higher fold changes in gene expression.

Table 3a: Relative Quantity of *ADCY* overexpression HEK293T cells				
Isoform Overexpressed	*ADCY 3* RQ	*ADCY 6* RQ	*ADCY 7* RQ	*ADCY 9* RQ
ADCY 3	13.55 (±1.15)	0.99 (±0.01)	0.99 (±0.05)	0.93 (±0.09)
ADCY 6	0.37 (±0.35)	142.23 (±27.40)	0.93 (±0.11)	0.99 (±0.05)
ADCY 7	0.34 (±0.32)	1.02 (±0.19)	4558.75 (±797)	0.86 (±0.07)
ADCY 9	0.46 (±0.43)	1.13 (±0.36)	1.23 (±0.04)	247.67 (±8.94)

Table 3b: Relative Quantity of *ADCY* overexpression sNF96.2 cells				
Isoform Overexpressed	*ADCY 3* RQ	*ADCY 6* RQ	*ADCY 7* RQ	*ADCY 9* RQ
ADCY 3	30.00(±1.70)	1.31(±0.06)	1.29(±0.05)	1.19(±)
ADCY 6	1.17(±0.12)	31.01(±5.17)	1.12(±0.03)	1.09(±)
ADCY 7	1.14(±0.01)	1.46(±0.13)	90.40(±17.9)	1.29(±)
ADCY 9	1.36(±0.12)	1.70(±0.61)	1.34(±0.33)	26.65(±)

Table 3c: Relative Quantity of *ADCY* overexpression ST88-14 cells				
Isoform Overexpressed	*ADCY 3* RQ	*ADCY 6* RQ	*ADCY 7* RQ	*ADCY 9* RQ
ADCY 3	318.33(±22.5)	1.63(±0.16)	1.99(±0.47)	1.34(±0.24)
ADCY 6	2.26(±0.30)	253.96(±26.7)	1.77(±0.22)	1.52(±0.19)
ADCY 7	3.09(±1.39)	2.64(±0.77)	1453.28(±760)	1.96(±0.69)
ADCY 9	2.05(±0.18)	1.67(±0.36)	1.47(±0.16)	337.37(±39.7)

Table3:(a-c) Relative quantities (RQ) of *ADCY* overexpression in various cell lines. Every isoform was significantly and selectively overexpressed in each cell line (ANOVA, p-value ≤ 0.001). In all cells lines *ADCY 7* was the most overexpressed compared to the other isoforms. ST88-14 (c) cells overexpressed most isoforms of *ADCY* more than the other cell lines. HEK293T cells had higher overexpression of *ADCY 7*. Standard deviations are shown in parentheses.

Overexpression of the intended *ADCY* isoforms was successful and statistically significant in all cell lines when tested with an ANOVA test (p-value ≤ 0.001). HEK293T cells responded the highest to *ADCY* 7. The least successful isoform in HEK293T cells, but still significant, was *ADCY* 3. In sNF96.2 cells, *ADCY 3, 6*, and *9* were overexpressed the most evenly over any other cell lines. ST88-14 cells were the most successfully overexpressed among *ADCY* isoforms *3, 6*, and *9*.

ADORA expression varies in response to *ADCY* isoform overexpression

Endogenous expression of *ADORA* was also measured using cycle threshold and expression varied between cell type and isoform (Figure 8). In HEK293T cells, *ADORA 1* was the least expressed isoform of any cell line. The other *ADORA* isoforms for HEK293T cells were moderately expressed. The MPNST cells showed slightly more variability in their values. In sNF96.2 cells, *ADORA 2A* and *3* had lower expression, whereas *ADORA 1* and *ADORA 2B* were more prominent. ADORA *2B* expression was significantly higher in expression in MPNST cell lines (ANOVA, p-value = 0.001).

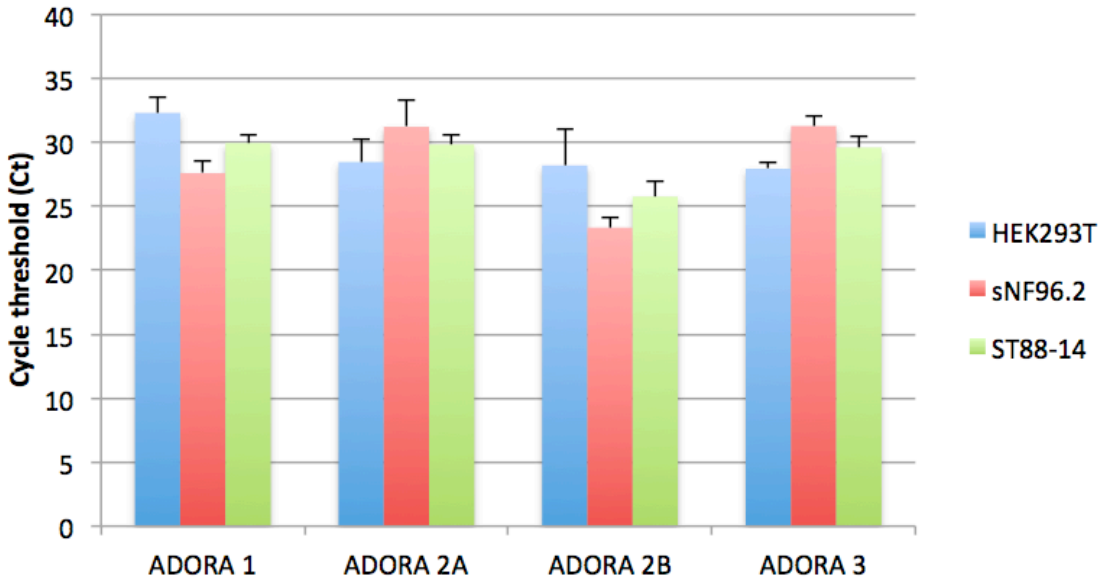

Figure 8: The cycle threshold (Ct) of endogenous *ADORA* expression in different cell lines. Each cell line was analyzed for endogenous expression of all four *ADORA* isoforms by Real-Time PCR. *ADORA 2B* Ct was significantly lower than other *ADORA* isoforms in both *NF1*-null MPNST cell lines. Ct values are inversely related to expression. Error bars represent standard deviation of samples.

The same technique of using the mock transfection to calculate RQ was used to measure *ADORA* with cells overexpressed with *ADCY*. *ADORA 1* expression in overexpressed *ADCY 9* cells showed significance, whereas other isoforms did not (Figure 9). In HEK293T cells, overexpressed *ADCY 9* cells had the highest *ADORA 1* expression; however, all cell lines had significant increases of *ADORA 1* when compared to their own mock transfections (p-value = 0.020, ANOVA).

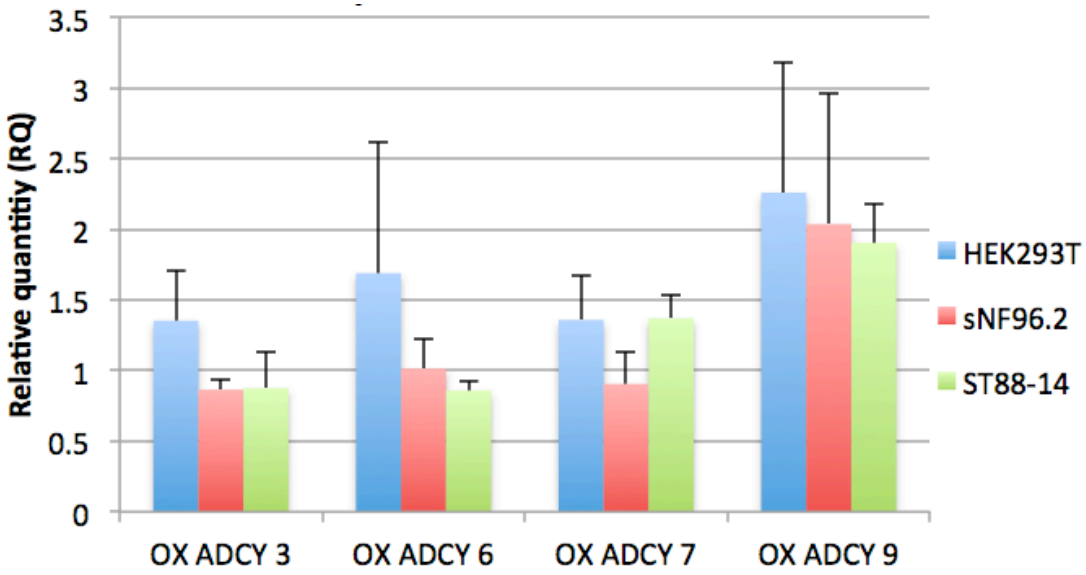

Figure 9: *ADORA 1* expression increased in response to *ADCY 9* overexpression. The RQ value of *ADORA 1* expression was calibrated using the mock transfection, which has an RQ value of one. RQ was nearly a two-fold increase for all cells, regardless of *NF1* genotype, when *ADCY 9* was overexpressed (OX). Error bars shown represent standard deviation.

ADORA 2A was significant, by some standards, between MPNST cells lines (p-value = 0.10, ANOVA) (Figure 10). The sNF96.2 cells had lower expression than the mock transfection sample between all *ADCY* isoforms. ST88-14 cells had approximately two-fold increases of RQ in isoforms *ADCY 3, 6*, and *7* and in overexpressed *ADCY 9* had nearly a three-fold increase in *ADORA 2A*.

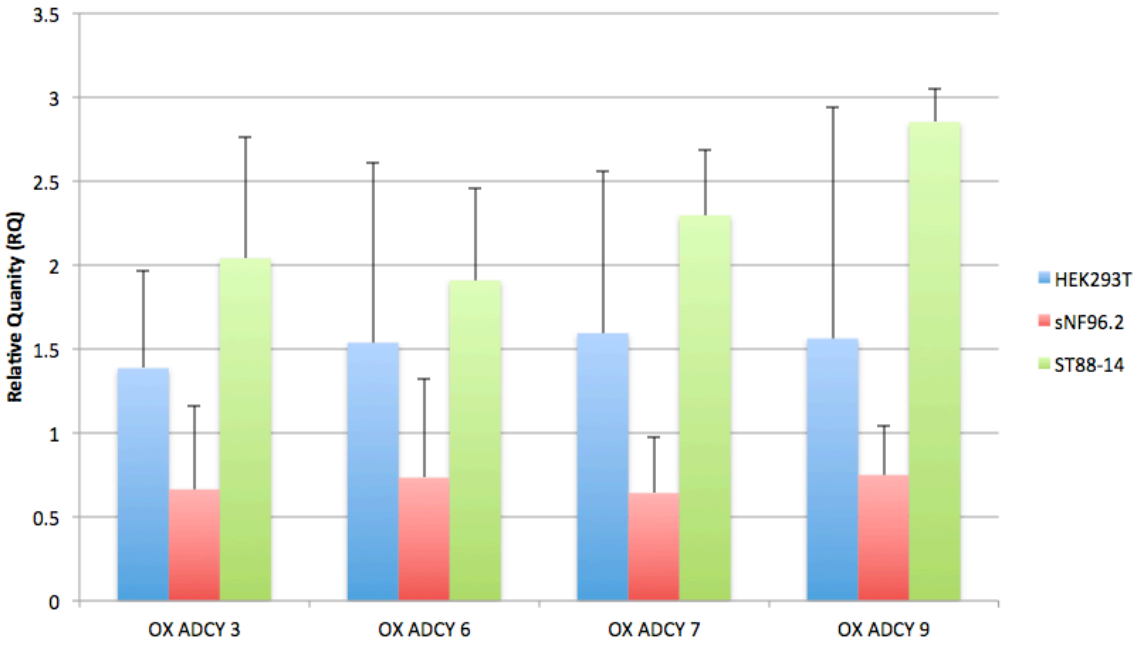

Figure 10: *ADORA 2A* expression increased in response to *ADCY 9* overexpression in *NF1*-null MPNST cells. When *NF1*-null MPNST cell lines were compared with one another there was borderline significance in the different RQ values (p-value = 0.10, ANOVA). ST88-14 cells overexpressed *ADORA 2A* in all isoforms to significant levels (when compared to its own mock transfection), whereas sNF96.2 cells experienced a decrease in expression for all *ADCY* isoforms. The HEK293T ($NF1^{+/+}$) cell line expressed slight overexpression in all *ADCY* isoforms. Error bars shown represent standard deviation.

ST88-14 cells showed significantly increased expression of *ADORA 2B* in response to overexpression of *ADCY 9* in ST88-14 cells (p-value = 0.017, ANOVA) (Figure 11). Whereas, overexpression of *ADCY 3, 6* and *7* had no effect on *ADORA 2B* expression. The sNF96.2 cell line showed no changes in *ADORA 2B* expression after overexpression of *ADCY*. Lastly, HEK293T cells had minor variation of *ADORA 2B* expression, but lacked significance.

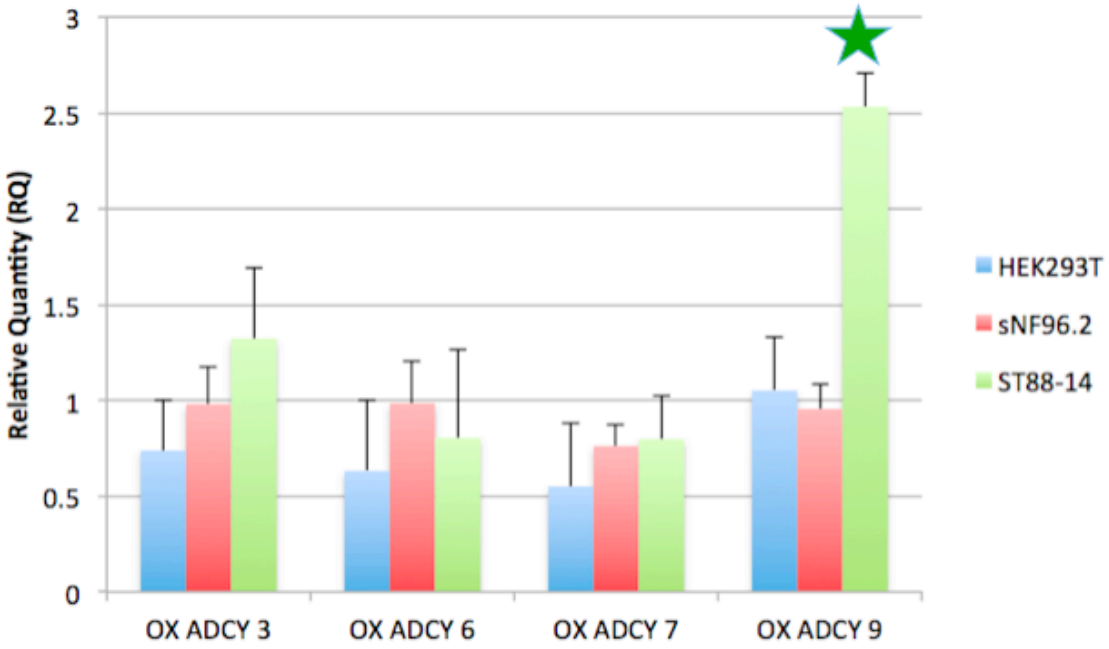

Figure 11: *ADORA 2B* expression significantly increased after *ADCY 9* overexpression in *NF1*-null MPNST cells. *ADORA 2B* showed significantly higher expression (p-value = 0.017, ANOVA) when ST88-14 cells were overexpressed with *ADCY 9*. The sNF96.2 cells ($NF1^{-/-}$) were consistent with the mock transfection even with overexpressed *ADCY*. The HEK293T ($NF1^{+/+}$) cell line was also not significantly changed from its mock transfection. Error bars shown represent standard deviation.

When *ADORA 3* was analyzed, there were significant differences between MPNST cell lines (Figure 12). ST88-14 cells experienced significant increases of *ADORA 3* when *ADCY 7* and *9* were overexpressed (p-value = 0.003, p-value = 0.03, ANOVA) and questionable significance with overexpression of *ADCY 3* (p-value = 0.13). In these cases, all experienced more than twice the expression compared to the mock and in the case of overexpressed *ADCY 9*, more than a four-fold increase in expression. The sNF96.2 cell line only increased expression of *ADORA 3* when *ADCY 9* was overexpressed and its expression decreased when *ADCY 3* and *7* were overexpressed. HEK293T cells did not change significantly when compared to their mock transfection.

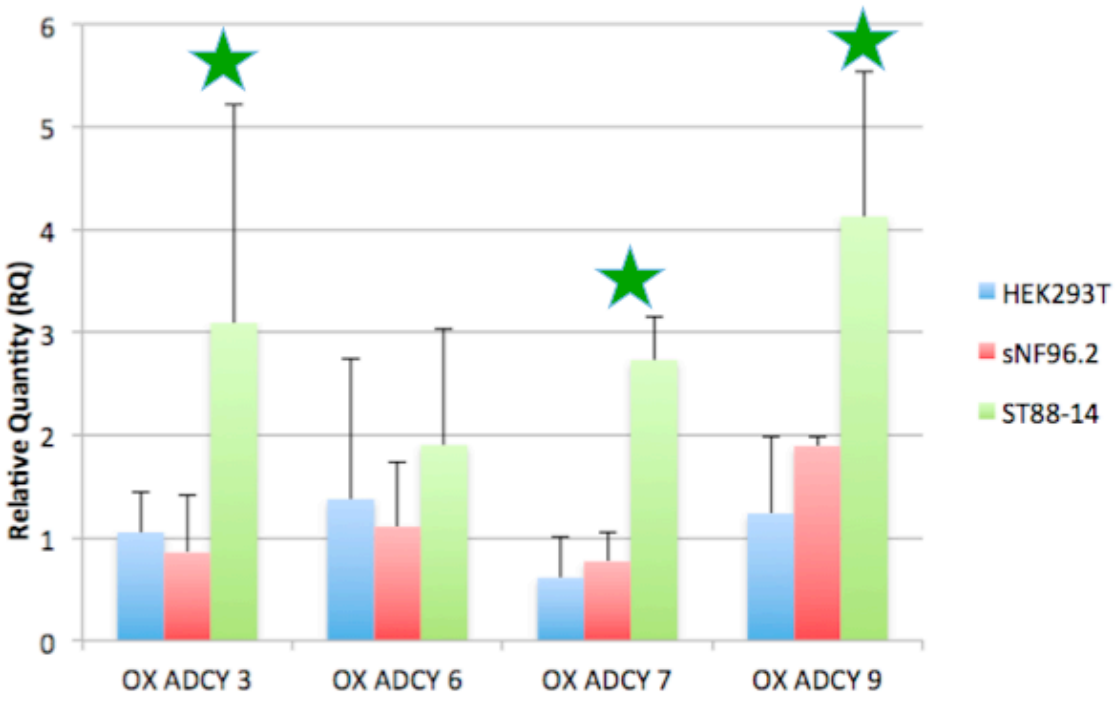

Figure 12: *ADORA 3* expression increased in response to *ADCY 9* overexpression in *NF1*-null MPNST cells. There were statistically significant differences in *ADORA 3* between MPNST cell lines**.** ST88-14 increased significantly when overexpressed with *ADCY 7* and *9*. Overexpression of *ADCY 3* had questionable significance in ST88-14 cells. The sNF96.2 cell line had an almost two-fold increase of *ADCY 9* expression. The HEK293T ($NF1^{+/+}$) cells did not change significantly. Error bars represent standard deviation.

Of the four overexpressed *ADCY* isoforms, overexpression of *ADCY 9* prompted the most significant changes in *ADORA* isoforms (Figure 13). All cell lines, regardless of genotype, overexpressed *ADORA 1,* approximately two-fold. In the ST88-14 cell line, *ADCY 9* overexpression prompted nearly a two-fold increase in expression in *ADORA 1*, but higher than two-fold overexpression in *ADORA 2A, 2B*, and *3*. The sNF96.2 cell line was near two-fold overexpression for *ADORA 1* and *3*.

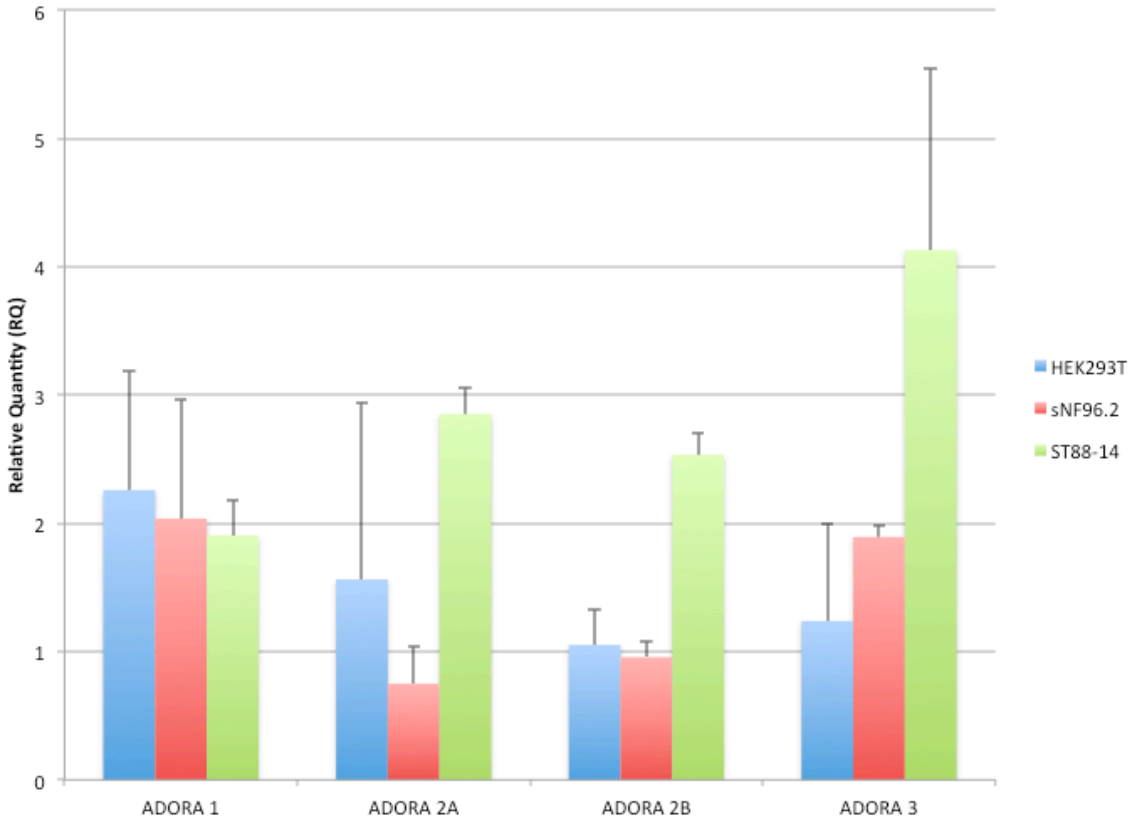

Figure 13: Overexpression of *ADCY 9* caused overexpression of every *ADORA* isoform in *NF1*-null MPNST cells. ST88-14 ($NF1^{-/-}$) cells experienced at least a two-fold overexpression of each *ADORA* isoform when *ADCY 9* was overexpressed. The sNF96.2 ($NF1^{-/-}$) cell line experienced an almost two-fold increased in *ADORA 3*. HEK293T ($NF1^{+/+}$) was only significantly overexpressed in *ADORA 1*, as were the other MPNST cell lines. Error bars represent standard deviation.

PKA activity altered in response to *ADCY* overexpression

Overexpressing *ADCY* isoforms changed PKA activity in a statistically significant manner in sNF96.2 cells. Overexpression of *ADCY 7* caused a significant decrease in PKA activity compared to other *ADCY* isoforms (p-value = 0.02, ANOVA) (Figure 14 and 15). Overexpression in HEK293T cells did not change PKA activity in a statistically significant manner. Both cell lines yielded lower PKA activity levels than the mock transfection (PKA Normalization Score = 1.0), suggesting that overexpressed *ADCY* decreased PKA activity.

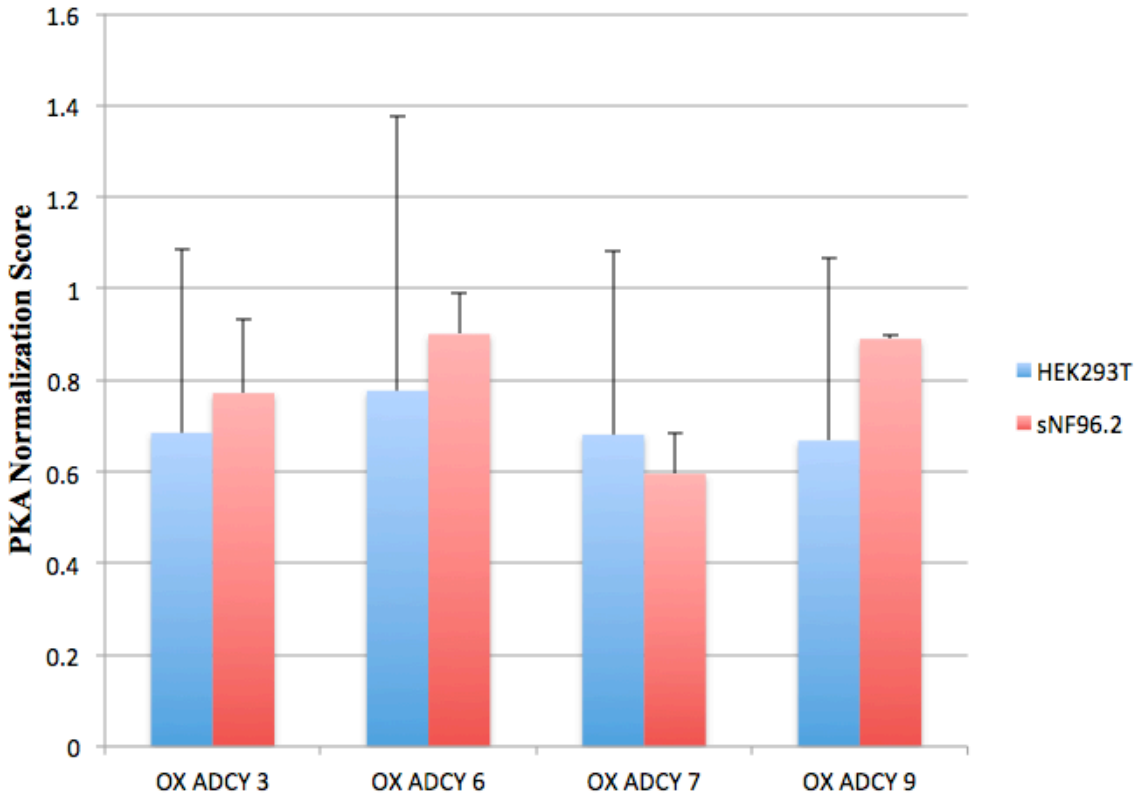

Figure 14: *ADCY* overexpression did not affect PKA activity. Overexpressing *ADCY* isoforms did not change phosphorylation in a statistically significant manner in cells with either *NF1* genotype. Error bars represent standard deviation.

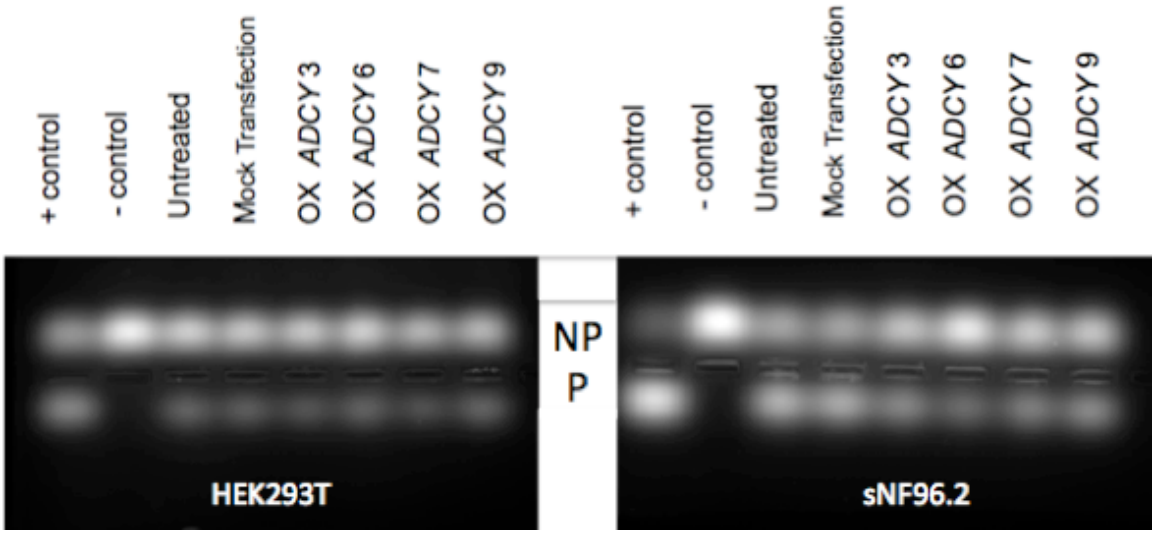

Figure 15: Representative gel images for PKA assay. On the left, PKA activity in a representative trial of HEK293T cells of overexpressed *ADCY*. On the right, PKA activity of a representative sample of sNF96.2 cells overexpressed with *ADCY*. Protein that was non-phosphorylated (NP) is located above each well and protein that was phosphorylated (P) is below each well.

DISCUSSION

The goal of this study, to dissect the relationship between ADCY, ADORA, and PKA in the context of mutated *NF1,* was met, and in the process has provided evidence that *NF1*-null cells have the ability to manipulate ADCY in two ways. In addition, more evidence has been collected that there is diversity within tumors of the same type of tissue. For example, when considering isoforms *ADCY 3, 6*, and *7,* HEK293T and sNF96.2 cells had more similar endogenous expression than the two MPNST cell lines. *ADCY 9* was the only isoform where the cycle threshold was within one unit of both MPNSTs, but HEK293T also measured in that same range (Figure 7). This suggests that *ADCY* expression is increased by more than a loss of function of *NF1*, possibly *ADORA* through an activated Ras pathway.

Endogenous *ADORA* expression within the three cell lines had more consistency between MPNSTs than *ADCY* (Figure 8). *ADORA2B* expression, in particular, was significantly higher than other isoforms. While overexpression of *ADCY 3, 6, 7*, and *9* was successful in all cell lines (Table 3), overexpressed *ADCY 6* did not create significant change in *ADORA* expression, whereas other *ADCY 3, 7*, and *9* did. In ST88-14 cells, *ADORA 2B* levels increased 2.5 times when *ADCY 9* was overexpressed (Figure 11). *ADORA 2B* is a direct stimulator of cAMP, independent of *NF1,* so this has particular importance when examining the *NF1*-null-cAMP relationship. In contrast, *ADORA 1* values increased significantly in all cell lines when *ADCY 9* was overexpressed. This is relevant because *ADORA 1* does not directly stimulate cAMP production, but in *NF1*-null cells there is an increase in RAS signaling. From RAS, PLC is signaled, which then directly stimulates IP3, *ADORA 1, 2B*, and *3*. *ADORA 2B* does stimulate *ADCY*;

therefore, this creates a positive feedback loop of increased cAMP (Figure 16). This provides supporting evidence that this may be how *NF1*-null cells increase their cAMP production so dramatically. Lastly, when *ADCY 3, 7* and *9* were overexpressed, *ADORA 3* increased in ST88-14 cells (Figure 12). While *ADORA 3* is not usually associated with the *ADCY* pathway, it is used in mast cell degranulation.

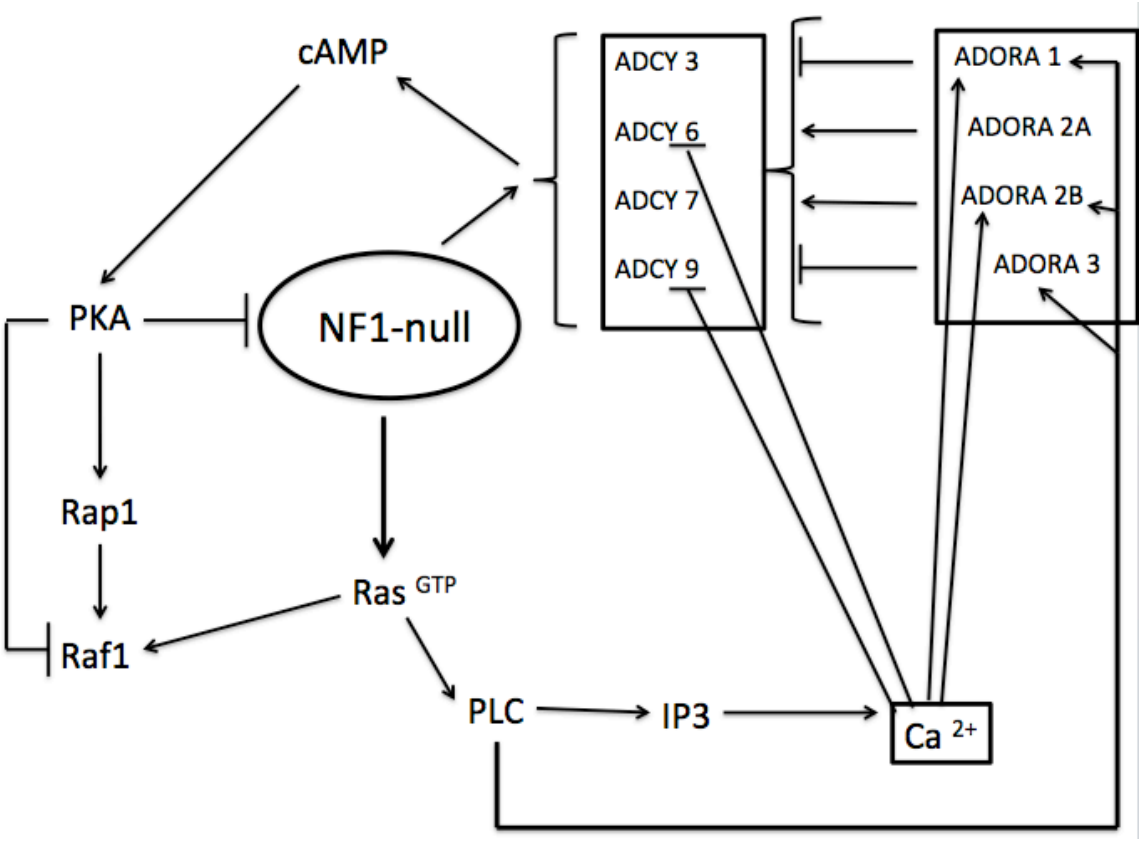

Figure 16: Feedback loop diagram of cell signaling caused by *NF1*-null cells. In a *NF1*-null cell, the Ras-PLC pathway causes more activity in ADORA 2B; therefore, increasing cAMP. Therefore, multiple pathways exist for increasing cAMP.

In order for MPNSTs to develop, the cellular environment that surrounds them must be haploinsufficient for *NF1* (Zhu *et al*. 2002), this includes the mast cells that invade the tumor. When mast cells degranulate they release cytokines, like tumor

necrosis factor-α (TNF-α), which promote tumor growth due to its ability to stimulate angiogenesis (Kessler *et al.* 1976). If *ADORA 3* expression increases, it is reasonable to assume that mast cell degranulation would increase; therefore, releasing more cytokines to promote the growth of MPNSTs. If a MPNST tumor grows that creates an opportunity for more cAMP production.

The results of the PKA assay indicate that overexpressing *ADCY 3, 6,* or *9* are not effective at altering PKA activity in a significant manner. However, the decreased activity of sNF96.2 cells when *ADCY 7* was overexpressed deserves attention. It was expected that overexpressed *ADCY* would increase PKA activity because cAMP is used to activate PKA. However, PKA is a known inhibitor of *ADCY 5* and *6*, this suggests that the reverse relationship may be true as well, except with *ADCY 7*. If overexpressed *ADCY 7* can change PKA activity in a MPNST cell line, this could influence the structure and function of neurofibromin. In addition, if PKA activity is changed, pathways like Rap1 and Raf1 (which can stimulate MEK) could be altered as well.

ST88-14 cells were not tested for changes in activity due to lacking PKA assay reagents. This is necessary to draw larger conclusions regarding the effects of overexpressing *ADCY* in MPNST cells, most notably *ADCY 7*. In addition, future studies could benefit from quantifying PKA activity by extracting sections of the gel and measuring via spectrophotometry. This would be a more objective method of measuring PKA activity than image software.

Based on these conclusions, it would be prudent to consider repeating this research with normal peripheral nerve tissue as a true experimental control and other

MPNST cells lines. While HEK293T cells do have functional *NF1*, they are not "healthy" cells and other MPNST cells lines would be helpful to learn where there are consistencies in expression. Futhermore, the sNF96.2 cells received from ATCC were highly passaged. This could have affected cell signaling in the cell line. Performing these experiments with a less passaged sNF96.2 cell line would be optimal.

Lastly, manipulating *ADORA* expression levels would also be a logical next step to provide more supporting evidence of the impact *ADCY* may have on *ADORA* expression and their feedback loops. Assays that identify specific portions of the signal cascade associated with *ADORA,* especially those involved in cell proliferation or apoptosis (i.e. cAMP, Ca^{2+}, ERK, MAP) would be sensible to study in the context of *NF1*-null MPNSTs. Understanding the signaling relationships in MPNSTs is essential to directing appropriate treatment.

REFERENCES

Ambrosini A, Tininini S, Barassi A, Racagni G, Sturani E, Zippel R. 2000. cAMP cascade leads to Ras activation in cortical neurons. Brain Res Mol Brain Res. 75(1):54-60.

Andersen, LB, Fountain, JW, Gutmann, DH, Tarlé, SA, Glover, TW, Dracopoli, NC, Housman, DE, Collins, FS. 1993. Mutations in the neurofibromatosis 1 gene in sporadic malignant melanoma cell lines. Nat. Genet. 3(2): 118-121.

Bahuau, M, Pelet, A, Vidaud, D, Lamireau, T, Le Bail, B, Munnich, A, Vidaud, M, Lyonnet, S, Lacombe, D. 2001. GDNF as a candidate modifier in a type 1 neurofibromatosis (NF1) enteric phenotype. (Letter) J. Med. Genet. 38: 638-643.

Barker D, Wright E, Nguyen K, Cannon L, Fain P, Goldgar D, Bishop DT, Carey J, Baty B, Kivlin J, et al. 1987. Gene for von Recklinghausen neurofibromatosis is in the pericentromeric region of chromosome 17. Science. 236(4805):1100-1102.

Barron V and Lou H. 2012. Alternative splicing the Neurofibromatosis type I pre-mRNA. Biosci Rep. 32(2): 131-138.

Basu TN, Gutmann DH, Fletcher JA, Glover TW, Collins FS, Downward J. 1992. Aberrant regulation of ras proteins in malignant tumour cells from type 1 neurofibromatosis patients. Nature. 356(6371):713-715.

Becker WM, Hardin J, Bertoni GP, Kleinsmith LJ. 2012. The World of the Cell. 8th ed. San Franscico (CA): Pearson Benjamin Cummings, Chapter 14: Signal transduction mechanisms II: messengers and receptors; p. 392-421.

Bollag G, McCormick F, Clark R. 1993. Characterization of full-length neurofibromin: tubulin inhibits Ras GAP activity. EMBO J. 12(5):1923-1927.

Borland G, Smith BO, Yarwood SJ. 2009. EPAC proteins transduce diverse cellular actions of cAMP. Br J Pharmacol. 158(1):70-86.

Broch OJ, Ueland PM. 1980. Regional and subcellular distribution of S-adenosylhomocysteine hydrolase in the adult rat brain. J Neurochem. 35(2):484-488.

Chiaradonna F, Balestrieri C, Gaglio D, Vanoni M. 2008. RAS and PKA pathways in cancer: new insight from transcriptional analysis. Front Biosci. 13:5257-5278.

Collins MG and Hourani SMO. 1993. Adenosine receptor subtypes. Trends in Pharmacological Sciences. 14(10): 361-366.

Cook SJ, McCormick F. 1993. Inhibition by cAMP of Ras-dependent activation of Raf. Science. 262(5136):1069-1072.

Cooper DMF and Tassasum VG. 2014. Adenylate cyclase - centered microdomains. Biochemical Journal. 462(2): 199-213.

Cryer PE, Jarett L, Kipnis DM. 1969. Nucleotide inhibition of adenyl cyclase activity in fat cell membranes. Biochim Biophys Acta. 177(3):586-590.

Dang I, De Vries GH. 2011. Aberrant cAMP metabolism in NF1 malignant peripheral nerve sheath tumor cells. Neurochem Res. 36(9):1697-1705.

da Rocha Lapa F, Junior SJM, Cerutti ML, Santos ARS. 2014. Chapter 4: Pharmacology of adenosine receptors and their signaling role in immunity and inflammation. Pharmacology and Therapeutics. InTechOpen.

Davis RL. 2000. Neurofibromin progress on the fly. Nature. 403(6772):846-847.

Defer N, Best-Belpomme M, Hanoune J. 2000. Tissue specificity and physiological relevance of various isoforms of adenylyl cyclase. Am J Physiol Renal Physiol. 279(3):F400-416.

Endo M, Ohashi K, Sasaki Y, Goshima Y, Niwa R, Uemura T, Mizuno K. 2003. Control of growth cone motility and morphology by LIM kinase and Slingshot via phosphorylation and dephosphorylation of cofilin. J Neurosci. 23(7):2527-2537.

Ercolino T, Lai R, Giache V, Melchionda S, Carella M, Delitala A, Mannelli M, Fanciulli G. 2014. Patient affected by neurofibromatosis type 1 and thyroid C-cell hyperplasia harboring pathogenic germ-line mutations in both NF1 and RET genes. Gene. 536(2):332-335.

Feng L, Yunoue S, Tokuo H, Ozawa T, Zhang D, Patrakitkomjorn S, Ichimura T, Saya H, Araki N. 2004. PKA phosphorylation and 14-3-3 interaction regulate the function of neurofibromatosis type I tumor suppressor, neurofibromin. FEBS Lett. 557(1-3):275-282.

Ferner RE, Huson SM, Thomas N, Moss C, Willshaw H, Evans DG, Upadhyaya M, Towers R, Gleeson M, Steiger C, et al. 2007. Guidelines for the diagnosis and management of individuals with neurofibromatosis 1. J Med Genet. 44(2):81-88.

Fredholm BB, AP IJ, Jacobson KA, Klotz KN, Linden J. 2001. International Union of Pharmacology. XXV. Nomenclature and classification of adenosine receptors. Pharmacol Rev. 53(4):527-552.

Guo HF, Tong J, Hannan F, Luo L, Zhong Y. 2000. A neurofibromatosis-1-regulated pathway is required for learning in Drosophila. Nature. 403(6772):895-898.

Harder A, Titze S, Herbst L, Harder T, Guse K, Tinschert S, Kaufmann D, Rosenbaum T, et al. Monozygotic Twins With Neurofibromatosis Type 1 (NF1) Display Differences in Methylation of *NF1* Gene Promoter Elements, 5' Untranslated region, Exon and Intron 1. 2010. Twin Research and Human Genetics. 13(6): 582-594.

Hsueh YP, Roberts AM, Volta M, Sheng M, Roberts RG. 2001. Bipartite interaction between neurofibromatosis type I protein (neurofibromin) and syndecan transmembrane heparan sulfate proteoglycans. J Neurosci. 21(11):3764-3770.

Izawa I, Tamaki N, Saya H. 1996. Phosphorylation of neurofibromatosis type 1 gene product (neurofibromin) by cAMP-dependent protein kinase. FEBS Lett. 382(1-2):53-59.

Jacobson KA, Gao ZG. 2006. Adenosine receptors as therapeutic targets. Nat Rev Drug Discovery. 5(3):247-264.

Jones GN, Tep C, Towns WH, 2nd, Mihai G, Tonks ID, Kay GF, Schmalbrock PM, Stemmer-Rachamimov AO, Yoon SO, Kirschner LS. 2008. Tissue-specific ablation of Prkar1a causes schwannomas by suppressing neurofibromatosis protein production. Neoplasia. 10(11):1213-1221.

Jones GN, Reilly KM. 2012. Neurofibromatosis Type 1. Berlin: Springer-Verlag. Chapter 19, Dissection of complex genetic and epigenetic interactions underlying NF1 cancer susceptibiity using mouse models; p. 287-304.

Kalff V, Shapiro B, Lloyd R, Sisson JC, Holland K, Nakajo M, Beierwaltes WH. 1982. The spectrum of pheochromocytoma in hypertensive patients with neurofibromatosis. Arch Intern Med. 142(12):2092-2098.

Kan Z, Jaiswal BS, Stinson J, Janakiraman V, Bhatt D, Stern HM, Yue P, Haverty PM, Bourgon R, Zheng J, et al. 2010. Diverse somatic mutation patterns and pathway alterations in human cancers. Nature. 466(7308):869-873.

Kessler DA, Langer RS, Pless NA, and Folkman J. 1976. Mast cells and tumor angiogenesis. International Journal of Cancer. 18(5): 703-709.

Kim HA, Ratner N, Roberts TM, Stiles CD. 2001. Schwann cell proliferative responses to cAMP and Nf1 are mediated by cyclin D1. J Neurosci. 21(4):1110-1116.

Kweh F, Zheng M, Kurenova E, Wallace M, Golubovskaya V, Cance WG. 2009. Neurofibromin physically interacts with the N-terminal domain of focal adhesion kinase. Mol Carcinog. 48(11):1005-1017.

Lazaro C, Gaona A, Ainsworth P, Tenconi R, Vidaud D, Kruyer H, Ars E, Volpini V, Estivill X. 1996. Sex differences in mutational rate and mutational mechanism in the NF1 gene in neurofibromatosis type 1 patients. Hum Genet. 98(6):696-699.

Linden J. 2001. Molecular approach to adenosine receptors: receptor-mediated mechanisms of tissue protection. Annu Rev Pharmacol Toxicol. 41: 775-787.

Legius E, Dierick H, Wu R, Hall BK, Marynen P, Cassiman JJ, Glover TW. 1994. TP53 mutations are frequent in malignant NF1 tumors. Genes Chromosomes Cancer. 10(4):250-255.

Ludwig MG, Seuwen K. 2002. Characterization of the human adenylyl cyclase gene family: cDNA, gene structure, and tissue distribution of the nine isoforms. J Recept Signal Transduct Res. 22(1-4):79-110.

Mawrin C, Kirches E, Boltze C, Dietzmann K, Roessner A, Stock-Schneider R. 2002. Immunohistochemical and molecular analysis of p53, RB, and PTEN in malignant peripheral nerve sheath tumors. Virchows Archiv. 440(6): 610-615.
Mischak H, Seitz T, Janosch P, Eulitz M, Steen H, Schellerer M, Philipp A, Kolch W. 1996. Negative regulation of Raf-1 by phosphorylation of serine 621. Mol Cell Biol. 16(10):5409-5418.

Mischak H, Seitz T, Janosch P, Eulitz M, Steen H, Schellerer M, Philipp A, Kolch W. 1996. Negative regulation of Raf-1 by phosphorylation of serine 621. Mol Cell Biol. 16(10):5409-5418.

Ostrom RS, Insel PA. 2004. The evolving role of lipid rafts and caveolae in G protein-coupled receptor signaling: implications for molecular pharmacology. Br J Pharmacol. 143(2):235-245.

Palmer TM, Stiles GL. 2000. Identification of threonine residues controlling the agonist-dependent phosphorylation and desensitization of the rat A(3) adenosine receptor. Mol Pharmacol. 57(3):539-545.

Pasmant E, Sabbagh A, Masliah-Planchon J, Ortonne N, Laurendeau I, Melin L, Ferkal S, Hernandez L, Leroy K, Valeyrie-Allanore L, Parfait B, Vidaud D, Bièche I, Lantieri L, Wolkenstein P, Vidaud M, Adamski H, Baumann-Morel C, Bastuji-Garin S, Bellanne C, Bieth E, Bousquet P, Brandt C, Balguerie X, Boudali L, Berbis P, Castelnau P, Chaix Y, Chevrant-Breton J, Collet E.2001. Role of noncoding RNA *ANRIL* in genesis of plexiform neurofibromas in neurofibromatosis type 1. J Natl Cancer Inst.103:1713–1722.

Perrone F, Da Riva L, Orsenigo M, Losa M, Jocolle G, Millefanti C, Pastore E, Gronchi A, Pierotti MA, Pilotti S. 2009. PDGFRA, PDGFRB, EGFR, and downstream signaling activation in malignant peripheral nerve sheath tumor. Neuro Oncol. 11(6):725-736.

Ratner N, Miller SJ. 2015. A RASopathy gene commonly mutated in cancer: the neurofibromatosis type 1 tumour suppressor. Nat Rev Cancer. 15(5):290-301.

Rosser T, Packer RJ. 2002. Neurofibromas in children with neurofibromatosis 1. J Child Neurol. 17(8):585-591; discussion 602-584, 646-551.

Sharmin S, Guan H, Williams AS, Yang K. 2012. Caffeine reduces 11beta-hydroxysteroid dehydrogenase type 2 expression in human trophoblast cells through the adenosine A(2B) receptor. PLoS One. 7(6):e38082.

Schmidt H, Taubert H, Wurl P, Bache M, Bartel F, Holzhausen HJ, Hinze R. 2001. Cytogenetic characterization of six malignant peripheral nerve sheath tumors: comparison of karyotyping and comparative genomic hybridization. 128(1):14-23.

Stenson PD, Mort M, Ball EV, Shaw K, Phillips A, Cooper DN. 2014. The Human Gene Mutation Database: building a comprehensive mutation repository for clinical and molecular genetics, diagnostic testing and personalized genomic medicine. Hum Genet. 133(1):1-9.

Sunahara RK, Dessauer CW, Gilman AG. 1996. Complexity and diversity of mammalian adenylyl cyclases. Annu Rev Pharmacol Toxicol. 36:461-480.

Tasken K, Solberg R, Zhao Y, Hansson V, Jahnsen T, Siciliano MJ. 1996. The gene encoding the catalytic subunit C alpha of cAMP-dependent protein kinase (locus PRKACA) localizes to human chromosome region 19p13.1. Genomics. 36(3):535-538.

The I, Hannigan GE, Cowley GS, Reginald S, Zhong Y, Gusella JF, Hariharan IK, Bernards A. 1997. Rescue of a Drosophila NF1 mutant phenotype by protein kinase A. Science. 276(5313):791-794.

Tokuo H, Yunoue S, Feng L, Kimoto M, Tsuji H, Ono T, Saya H, Araki N. 2001. Phosphorylation of neurofibromin by cAMP-dependent protein kinase is regulated via a cellular association of N(G),N(G)-dimethylarginine dimethylaminohydrolase. FEBS Lett. 494(1-2):48-53.

Upadhyaya M, Huson SM, Davies M, Thomas N, Chuzhanova N, Giovannini S, Evans DG, Howard E, Kerr B, Griffiths S, et al. 2007. An absence of cutaneous neurofibromas associated with a 3-bp inframe deletion in exon 17 of the NF1 gene (c.2970-2972 delAAT): evidence of a clinically significant NF1 genotype-phenotype correlation. Am J Hum Genet. 80(1):140-151.

Wallace MR, Marchuk DA, Andersen LB, Letcher R, Odeh HM, Saulino AM, Fountain JW, Brereton A, Nicholson J, Mitchel AL, Brownstein BH, and Collins FS. 1990. Type 1 Neurofibromatosis Gene: Identification of a Large Transcript Disrupted in Three NF1 Patients. Science. 249 (4965): 181-186.

Wang HF, Shih YT, Chen CY, Chao HW, Lee MJ, Hsueh YP. 2011. Valosin-containing protein and neurofibromin interact to regulate dendritic spine density. J Clin Invest. 121(12):4820-4837.

Williams VC, Lucas J, Babcock MA, Gutmann DH, Korf B, Maria BL. 2009. Neurofibromatosis type 1 revisited. Pediatrics. 123(1):124-133.

Xu GF, O'Connell P, Viskochil D, Cawthon R, Robertson M, Culver M, Dunn D, Stevens J, Gesteland R, White R, et al. 1990. The neurofibromatosis type 1 gene encodes a protein related to GAP. Cell. 62(3):599-608.

Yang L, Jackson E, Woerner BM, Perry A, Piwnica-Worms D, Rubin JB. 2007. Blocking CXCR4-mediated cyclic AMP suppression inhibits brain tumor growth in vivo. Cancer Res. 67(2):651-658.

Zachary I. 1997. Focal adhesion kinase. Int J Biochem Cell Biol. 29(7):929-934.

Zehavi C, Romano A, Goodman RM. 1986. Iris (Lisch) nodules in neurofibromatosis. Clin Genet. 29(1):51-55.

Zhu Y, Ghosh P, Charnay P, Burns DK, Parada LF. 2002. Neurofibromas in NF1: Schwann cell origin and role of environment. Science. 296(5569): 920-922.